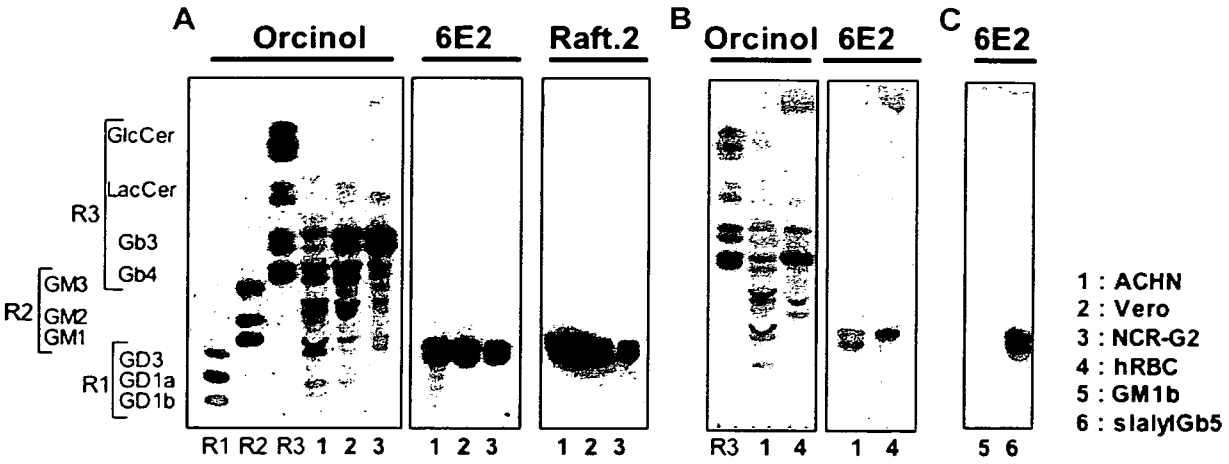

Fig. 1. TLC immunostaining of GSLs prepared from cultured cells and hRBCs. GSLs extracted from cultured cells and hRBCs or purified GSLs were separated by TLC in a solvent system of chloroform/methanol/water containing 0.2% $CaCl_2$ (5:4:1, v/v/v). Plates were chemically stained with orcinol-sulfurnic acid or were immunostained with 6E2 and Raft.2. Lane 1, ACHN; Lane 2, Vero; Lane 3, NCR-G2; Lane 4, hRBCs; Lane 5, GM1b; Lane 6, sialylGb5. Reference markers used were disialosyl gangliosides of GD3, GD1a, and GD1b (R1), monosialosyl gangliosides of GM3, GM2, and GM1 (R2), and neutral GSLs of GlcCer, LacCer, Gb3, and Gb4 (R3). The nomenclature for GSLs follows the recommendations [11] of the IUB, and the ganglioside nomenclature of Svennerholm [12] was used.

Mab. The 80 kDa protein might be associated with sialylGb5 in NCR-G3 cells and thus co-immunoprecipitated by 6E2.

Comparison of reactivity to sialyl Gb5 between 6E2 and MC813-70

MC813-70 established by immunizing with human EC cell lines has been most widely used as an anti-SSEA-4 antibody (mouse IgG_3, κ) [14]. Therefore we compared the reactivities of the Mabs 6E2 and MC813-70 by flow cytometry and dot-blot immunostaining. The fluorescence intensity obtained with 6E2 was stronger than that with MC813-70 in each cell line and hRBCs (Fig. 2A). A recent flow cytometric study showed that MC813-70 strongly stains hRBCs, but other anti-sialyGb5 Mabs do not [15]. However, our data indicate that 6E2 is more reactive than MC813-70. Next we compared the reactivity of the two

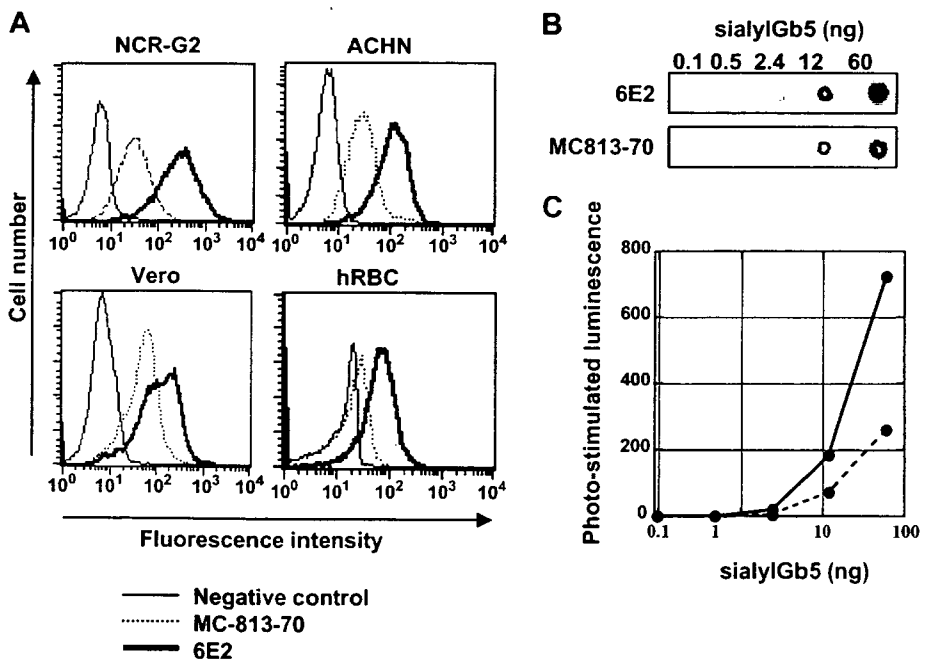

Fig. 2. Reactivity of 6E2 and MC813-70 with sialylGb5. (A) Flow cytometric analysis of SSEA-4-positive cells with 6E2. NCR-G2 cells, ACHN cells, Vero cells, and hRBCs were stained with 6E2 (bold line) or MC813-70 (dotted line) and with a FITC-conjugated secondary antibody and analyzed by flow cytometry. (B) An image of the dot-blot immunostaining of sialylGb5 obtained with a LAS-1000 luminescent imaging analyzer. (C) Measurement of antibodies bound (6E2: solid line, MC813-70: broken line).

Mabs with that of sialylGb5 by dot-blot immunostaining. Serially diluted sialylGb5 was dot-blotted onto a PVDF membrane, and the membrane was immunostained with the two Mabs. Both 6E2 and MC813-70 bound to more than 12 ng of sialylGb5, but the signals induced by 6E2 were stronger than those induced by MC813-70 (Fig. 2B,C). Thus, in addition to the flow cytometric analysis, the reactivity of 6E2 with sialylGb5 was stronger than that of MC813-70 by dot-blot immunostaining.

SSEA-4 Immunostaining of cynomolgus monkey ES cells

To confirm whether Mab 6E2 reacts with SSEA-4 on monkey ES cells, we performed an indirect immunofluorescence staining of cynomolgus monkey ES cells with Mab 6E2 and MC813-70. Mab 6E2 reacted with monkey ES cells (Fig. 3A) as well as MC-813-70 did (Fig. 3B). No difference in staining patterns of SSEA-4 between the two Mabs was observed. Mab 6E2 certainly stained SSEA-4 on monkey ES cells.

SSEA-4 immunostaining of "living" mouse preimplantation embryos without fixation

During early embryogenesis in mice, SSEA-4 had been reported to be expressed in fertilized eggs with levels gradually increasing to the morula stage and then decreasing [5]. Thus we examined the expression and distribution of SSEA-4 in preimplantation mouse embryos by immunostaining with both 6E2 and MC813-70. Both Mabs evenly stained the whole surface membranes of fixed mouse embryos, and no difference in staining pattern between the two was observed (data not shown). In order to perform a time-course of SSEA-4 distribution in a viable state, we performed immunostaining of preimplantation embryos without fixation.

3D-images of the 6E2 staining pattern obtained by confocal laser scanning microscopic observation clearly showed the localization of SSEA-4 on mouse preimplantation embryos. Two-cell embryos showed patches of SSEA-4 over the whole surface membrane with some accumulation at the interface between blastomeres (Fig. 4A). In 8-cell embryos, the amount accumulated at interfaces was further increased, as if planer membranes separate each blastomere, and some large patches were internalized but others were left on the surface membranes (Fig. 4B). The amount of SSEA-4 concentrated at the interfaces in morula was not as significant as in 8-cell embryos but still clearly observed and some patches were internalized (Fig. 4C).

2D-images of embryos stained with 6E2 showed a marked accumulation of SSEA-4 at the interfaces between blastomeres (Fig. 4D–F). These results suggest that sialylGb5 actively moves during development and tends to accumulate where blastomeres come into contact with each other.

Interestingly, however, the staining pattern of SSEA-4 using MC813-70 was different from that using 6E2. MC813-70 evenly stained the surface and the interface between blastomeres of 2-cell embryos with patches (Fig. 4G), and the amount of SSEA-4 at interfaces was not significant (Fig. 4J). In 8-cell embryos, there were patches of SSEA-4 in the central area of the outer surface of each blastomere (Fig. 4H, indicated by arrows), but the 2D-image showed that clustering also occurred at surfaces facing blastocoels (Fig. 4K, indicated by arrowheads). In morula embryos, SSEA-4 was distributed on the surface in patches and was enriched at the boundaries between blastomeres on the outer surface (Fig. 4I,L).

It remains unclear why the pattern of staining of mouse preimplantation embryos differs between 6E2 and MC813-70. The composition of fatty acids in GSLs influences the binding of antibodies [16,17] or bacterial toxins [18]. SialylGb5 recognized by the two MAbs might differ in composition of fatty acids, resulting in different immunostaining patterns. It was reported that the clustering of sialylGb5 by a Mab induces the activation of sialylGb5-associated kinases in raft microdomains of human mammary carcinoma cells, leading to downstream signaling [19,20]. The clustering of sialyGb5 by 6E2 on preimplantation mouse embryos may also induce the activation of some kinases, followed by downstream signaling. Recently, Comisky et al. suggested that lipid rafts and their associated molecules are spatiotemporally positioned to play a critical role in preimplantation developmental events [21]. The patches or clusters of sialylGb5 shown in our study suggest the presence of lipid rafts containing sialylGb5 on mouse embryos.

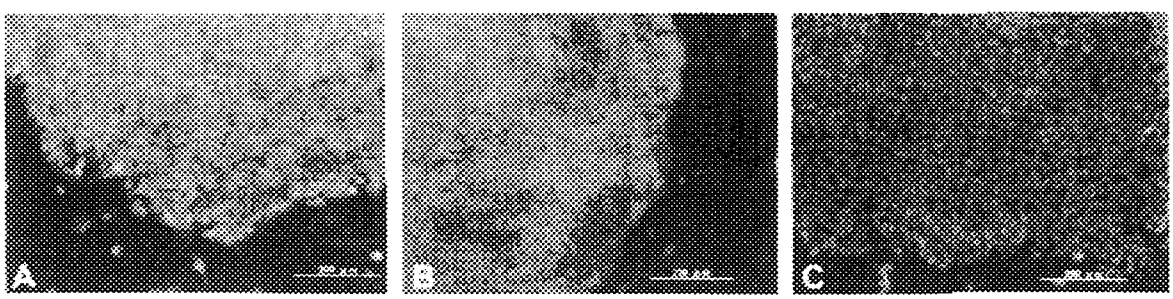

Fig. 3. Indirect immunostaining of cynomolgus monkey ES cell line CMK-6 with 6E2 and MC813-70. The CMK-6 cells were stained with 6E2 (A), MC813-70 (B), or isotype-matched mouse IgG (C), and visualized with secondary antibodies (green), followed by counterstaining of nuclei with DAPI (blue). Scale bars = 200 μm.

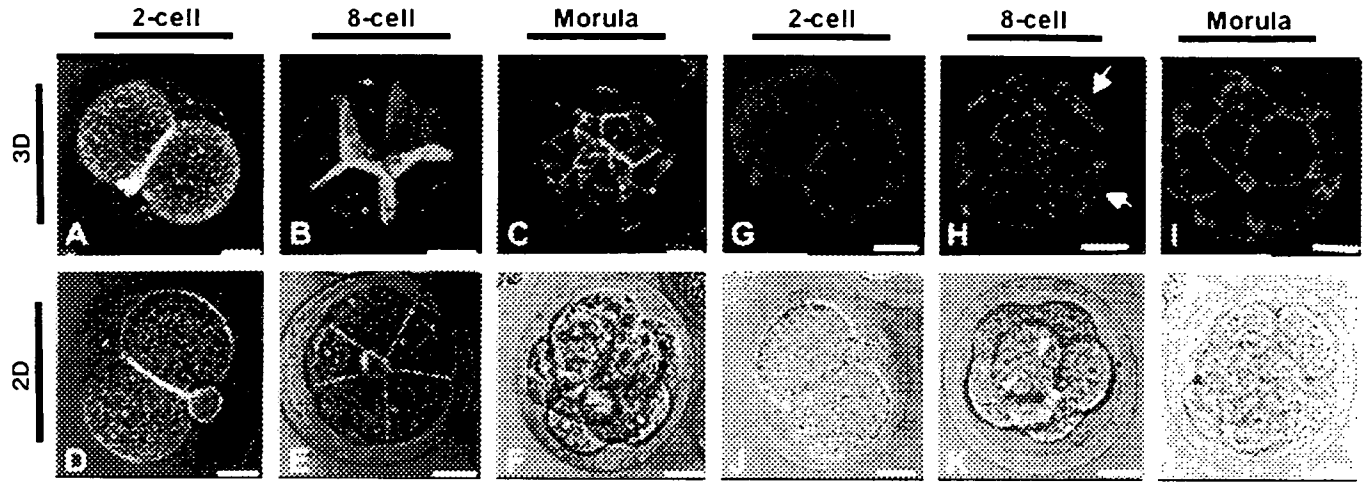

Fig. 4. Immunostaining of SSEA-4 on mouse preimplantation embryos with 6E2 and MC813-70. The embryos at the 2-cell (A, D, G, J), the 8-cell (B, E, H, K), and the morula (C, F, I, L) stages were stained with 6E2 (green) or MC813-70 (red). The panels designated 3D (A, B, C, G, H, I) are three-dimensional images reconstructed by stacking optical slice images using LSM software and the panels designated 2D (D, E, F, J, K, L) are an overlay of a fluorescent image and a differential interference contrast micrograph. Scale bars = 20 μm.

6E2 has high affinity for sialylGb5 and can be effectively conjugated with fluorescence reagents, leading to excellent staining of SSEA-4 in the surface membrane of "living" mouse preimplantation embryos. 6E2 should be of use for research into lipid rafts in early development and of great advantage for the characterization of ES cells and EC cells.

Acknowledgments

We thank S. Yamauchi for her excellent secretarial work. This work was supported in part by grants from CREST of JST and the 3rd. term comprehensive 10-year-strategy for cancer control, Research on Children and Families, Research on Human Genome Tailor made and Research on Publicly Essential Drugs and Medical Devices, Health and Labour Sciences Research Grants from the Ministry of Health, Labour and Welfare of Japan and a grant from The Japan Leukemia Research Field.

References

[1] B. Mintz, K. Illmensee, Normal genetically mosaic mice produced from malignant teratocarcinoma cells, Proc. Natl. Acad. Sci. USA 72 (1975) 3585–3589.

[2] P.W. Andrews, I. Damjanov, D. Simon, G.S. Banting, C. Carlin, N.C. Dracopoli, J. Fogh, Pluripotent embryonal carcinoma clones derived from the human teratocarcinoma cell line Tera-2. Differentiation in vivo and in vitro, Lab Invest. 50 (1984) 147–162.

[3] J.F. Jun-ichi Hata, Eizaburo Ishii, Akihiro Umezawa, Yasuo Kokai, Yoshie Matsubayashi, Hiroshi Abe, Satoru Kusakari, Haruto Kikuchi, Taketo Yamada, Tatsuya Maruyama, Differntiation of human germ cell tumor cells *in vivo* and *in vitro*, Acta Histochem. Cytochem. 25 (1992) 563–576.

[4] J.S. Draper, C. Pigott, J.A. Thomson, P.W. Andrews, Surface antigens of human embryonic stem cells: changes upon differentiation in culture, J. Anat. 200 (2002) 249–258.

[5] T. Muramatsu, H. Muramatsu, Carbohydrate antigens expressed on stem cells and early embryonic cells, Glycoconj. J. 21 (2004) 41–45.

[6] T. Nakano, A. Umezawa, H. Abe, N. Suzuki, T. Yamada, S. Nozawa, J. Hata, A monoclonal antibody that specifically reacts with human embryonal carcinomas, spermatogonia and oocytes is able to induce human EC cell death, Differentiation 58 (1995) 233–240.

[7] M. Yamamoto, N. Tase, T. Okuno, Y. Kondo, S. Akiba, N. Shimozawa, K. Terao, Monitoring of gene expression in differentiation of embryoid bodies from cynomolgus monkey embryonic stem cells in the presence of bisphenol A, J. Toxicol. Sci. 32 (2007) 301–310.

[8] Y.U. Katagiri, K. Ohmi, C. Katagiri, T. Sekino, H. Nakajima, T. Ebata, N. Kiyokawa, J. Fujimoto, Prominent immunogenicity of monosialosyl galactosylgloboside, carrying a stage-specific embryonic antigen-4 (SSEA-4) epitope in the ACHN human renal tubular cell line-a simple method for producing monoclonal antibodies against detergent-insoluble microdomains/raft, Glycoconj. J. 18 (2001) 347–353.

[9] Y.U. Katagiri, N. Kiyokawa, K. Nakamura, H. Takenouchi, T. Taguchi, H. Okita, A. Umezawa, J. Fujimoto, Laminin binding protein, 34/67 laminin receptor, carries stage-specific embryonic antigen-4 epitope defined by monoclonal antibody Raft:2, Biochem. Biophys. Res. Commun. 332 (2005) 1004–1011.

[10] K. Nakamura, Y. Hashimoto, M. Suzuki, A. Suzuki, T. Yamakawa, Characterization of GM1b in mouse spleen, J. Biochem. (Tokyo) 96 (1984) 949–957.

[11] The nomenclature of lipids (recommendations 1976). IUPAC-IUB Commission on Biochemical Nomenclature, J. Lipid. Res. 19 (1978) 114–128.

[12] L. Svennerholm, Designation and schematic structure of gangliosides and allied glycosphingolipids, Prog. Brain Res. 101 (1994) XI–XIV.

[13] L.L. Cooling, K. Kelly, Inverse expression of P(k) and Luke blood group antigens on human RBCs, Transfusion 41 (2001) 898–907.

[14] L.H. Shevinsky, B.B. Knowles, I. Damjanov, D. Solter, Monoclonal antibody to murine embryos defines a stage-specific embryonic antigen expressed on mouse embryos and human teratocarcinoma cells, Cell 30 (1982) 697–705.

[15] L. Cooling, D. Hwang, Monoclonal antibody B2, a marker of neuroendocrine sympathoadrenal precursors, recognizes the Luke (LKE) antigen, Transfusion 45 (2005) 709–716.

[16] K. Iwabuchi, I. Nagaoka, Lactosylceramide-enriched glycosphingolipid signaling domain mediates superoxide generation from human neutrophils, Blood 100 (2002) 1454–1464.

[17] K. Iwabuchi, Y. Zhang, K. Handa, D.A. Withers, P. Sinay, S. Hakomori, Reconstitution of membranes simulating "glycosignaling

domain" and their susceptibility to lyso-GM3, J. Biol. Chem. 275 (2000) 15174–15181.
[18] A. Kiarash, B. Boyd, C.A. Lingwood, Glycosphingolipid receptor function is modified by fatty acid content. Verotoxin 1 and verotoxin 2c preferentially recognize different globotriaosyl ceramide fatty acid homologues, J. Biol. Chem. 269 (1994) 11138–11146.
[19] W.F. Steelant, Y. Kawakami, A. Ito, K. Handa, E.A. Bruyneel, M. Mareel, S. Hakomori, Monosialyl-Gb5 organized with cSrc and FAK in GEM of human breast carcinoma MCF-7 cells defines their invasive properties, FEBS Lett. 531 (2002) 93–98.
[20] S. Van Slambrouck, W.F. Steelant, Clustering of monosialyl-Gb5 initiates downstream signalling events leading to invasion of MCF-7 breast cancer cells, Biochem. J. 401 (2007) 689–699.
[21] M. Comiskey, C.M. Warner, Spatio-temporal localization of membrane lipid rafts in mouse oocytes and cleaving preimplantation embryos, Dev. Biol. 303 (2007) 727–739.

International Journal of
HEMATOLOGY

Characterization of Monocyte-Macrophage–Lineage Cells Induced from CD34+ Bone Marrow Cells In Vitro

Kyoko Suzuki,[a,b] Nobutaka Kiyokawa,[a] Tomoko Taguchi,[a] Hisami Takenouchi,[a] Masahiro Saito,[b] Toshiaki Shimizu,[b] Hajime Okita,[a] Junichiro Fujimoto[a]

[a]*Department of Developmental Biology, National Research Institute for Child Health and Development, Tokyo, Japan;* [b]*Department of Pediatrics, Juntendo University, School of Medicine, Tokyo, Japan*

Received November 15, 2006; received in revised form February 13, 2007; accepted February 19, 2007

Abstract

We characterized the expression of cell surface antigens and cytokine-secreting ability of monocyte-macrophage–lineage cells induced in vitro from CD34+ bone marrow cells. After cultivation for 3 weeks, we observed 2 distinct cell fractions: a floating small, round cell fraction and an adherent large, protruding cell fraction. Both cell fractions expressed myelocyte-monocyte–lineage antigens, but mature-macrophage markers such as CD206 were expressed only by the adherent cells. An assessment of cells cultured for 5 weeks revealed spontaneous secretion of interleukin 8 (IL-8) and IL-6, and lipopolysaccharide (LPS)-induced tumor necrosis factor α (TNF-α) secretion in both fractions, but only the adherent cell fraction secreted IL-10 after LPS stimulation. In contrast, both fractions of cells cultured for 3 weeks spontaneously secreted low levels of IL-8, but none of the other cytokines. Upon LPS stimulation, the cells secreted IL-6 and TNF-α, but not IL-10. We also assessed the effect of granulocyte colony-stimulating factor (G-CSF) pretreatment on TNF-α secretion by each cell fraction and found that G-CSF reduced TNF-α secretion only in the adherent fraction of cells cultured for 3 weeks. Monocyte-macrophage–lineage cells induced in vitro should provide an ideal model for functional analysis of monocyte-macrophage cells.
Int J Hematol. 2007;85:384-389. doi: 10.1532/IJH97.06213

Key words: Monocyte-macrophage lineage; Antigen; Cytokine; Expression

1. Introduction

The mononuclear phagocyte system includes a widely distributed family of related cells (such as peripheral blood monocytes, macrophages, Kupffer cells, dendritic cells, osteoclasts, and microglia) that exhibit highly specialized functions. Macrophages resident in a number of tissues act as professional phagocytes and remove pathogens or apoptotic cells [1]. Dendritic cells are specialized to capture and present antigens, initiating the immune response through naive T-cell activation [2]; dendritic cells are also implicated in maintaining tolerance to self antigens [3]. Osteoclasts, multinucleated bone-resorbing cells found in the vicinity of bone, play an essential role in bone remodeling as well as in regulating calcium homeostasis [4]. Microglia represent a unique category of mononuclear phagocytes distributed throughout the central nervous system [5], and in addition to their role as the immune effectors of the central nervous system, they perform nonimmunologic functions, including the production of neurotrophic factors and glutamate uptake [6,7].

The mononuclear phagocytic cells are believed to originate from hematopoietic stem cells in the bone marrow (BM). In the conventional view, monocytes that develop in the BM are released into the circulation and then enter the tissues to become resident macrophages and other mononuclear phagocytic cells [8,9]. Consistent with this view, Kennedy and Abkowitz demonstrated in a mouse transplantation system that more mature monocytes give rise to tissue macrophages, including alveolar macrophages in the lung and Kupffer cells in the liver [10]. The results of a number of studies have suggested, however, that the mechanism of mononuclear phagocytic cell development is more complicated. One intriguing possibility is that less mature marrow-derived cells, such as macrophage colony-forming units, enter

Correspondence and reprints requests: Nobutaka Kiyokawa, MD, PhD, Department of Developmental Biology, National Research Institute for Child Health and Development, 2-10-1, Okura, Setagaya-ku, Tokyo 154-8535, Japan; 81-3-3417-2496; fax: 81-3-3417-2496 (e-mail: nkiyokawa@nch.go.jp).

the tissues and differentiate into macrophages [11]. Prior studies have shown that tissue macrophages divide in situ, indicating that these cells are responsible for the renewal and expansion of this population [12-14].

The functional and phenotypic heterogeneity within the phagocyte system may be evidence of the differentiation plasticity of a common progenitor, but the details of the developmental pathways leading to the maturation of mononuclear phagocytic cells are still unclear. In vitro culture systems in which mature mononuclear phagocytic cells are induced from hematopoietic stem cells or monocyte precursors have been employed in a number of studies to clarify the molecular mechanism of phagocytic cell development. For example, monocyte-macrophage–lineage cells can be induced from CD34+ cord blood hematopoietic stem cells by liquid culture with cytokines [15] and by cocultivation with BM stromal cell lines in the presence of cytokines [16]. BM progenitors have recently been identified by their ability to differentiate into dendritic cells or osteoclasts, depending on whether they are exposed to RANKL in combination with granulocyte-macrophage colony-stimulating factor (GM-CSF) or M-CSF [17].

To evaluate the usefulness of monocyte-macrophage–lineage cells as a source for an in vitro model for the functional analysis of a monocytic phagocyte system, we analyzed the immunophenotype of and cytokine production by monocyte-macrophage–lineage cells induced from CD34+ BM cells in vitro. In this study, we showed that several distinct developmental stage–related subpopulations are present in monocyte-macrophage–lineage cells induced from CD34+ BM cells in vitro.

2. Materials and Methods

2.1. Cells and Reagents

Human BM CD34+ cells from Cambrex Bio Science Walkersville (Walkersville, MD, USA) were used. The cells had been isolated from human tissue after informed consent had been obtained. Recombinant human cytokines were purchased from PeproTech (London, UK). Fluorescently conjugated monoclonal antibodies were purchased from Beckman Coulter (Westbrook, MA, USA). Unless otherwise indicated, all other chemical reagents were obtained from Wako Pure Chemical Industries (Osaka, Japan).

2.2. Cultures

Monocyte-macrophage–lineage cells were induced by incubating human BM CD34+ cells (1×10^5 cells/well of a 6-well plate) at 37°C under 5% carbon dioxide in 5 mL of 10% (vol/vol) fetal calf serum (Sigma-Aldrich, St. Louis, MO, USA) containing RPMI 1640 medium (Sigma-Aldrich) supplemented with a cytokine mixture consisting of interleukin 3 (IL-3) (20 ng/mL), IL-6 (20 ng/mL), M-CSF (100 ng/mL), GM-CSF (20 ng/mL), and Flt-3 ligand (100 ng/mL) [15,18]. Every week, half of the medium was replaced with fetal calf serum–containing medium supplemented with M-CSF alone. After 3 weeks of cultivation, the medium was completely replaced with the medium supplemented with M-CSF alone, and the cells were cultured for another 2 weeks. At the end of 5 weeks of cultivation, the floating cells in the medium were collected, and the adherent cells were harvested with 0.25% trypsin plus 0.02% EDTA (Immuno-Biological Laboratories Co, Gunma, Japan). These 2 cell fractions were used for further examination.

For the histology studies, cells were harvested and immobilized on glass slides with Cytospin 2 (Shandon, Pittsburgh, PA, USA). After Giemsa staining, cell morphology was assessed by light microscopy (BX-61; Olympus, Tokyo, Japan). Cells were tested for cytokine secretion by exposing the cells to G-CSF and stimulating them with lipopolysaccharide (LPS) (Sigma-Aldrich) for 24 hours, as described previously [19].

2.3. Reverse Transcriptase–Polymerase Chain Reaction Analysis

Total RNA was extracted from cultured human BM cells, and complementary DNA (cDNA) was generated with an RNeasy Mini Kit (Qiagen, Valencia, CA, USA) and a First-Strand cDNA Synthesis Kit (Pfizer, Uppsala, Sweden). cDNA synthesized from 150 ng of total RNA was used as a template for one amplification reaction. The following sets of primers were used: 5′-ttattacccctccttcagacac-3′ (sense) and 5′-aagtctggaaacatctggagagag-3′ (antisense), for amplification of a 347-bp fragment of human tumor necrosis factor α (TNF-α) cDNA; 5′-aagtggtgttctccatgtcc-3′ (sense) and 5′-gagcgaatgacagagggttt-3′ (antisense), for amplification of a 664-bp fragment of human IL-1β cDNA; and 5′-gctggaggactttaagggtt-3′ (sense) and 5′-cccagatccgattttggaga-3′ (antisense), for amplification of a 394-bp fragment of human IL-10 cDNA. The set of primers for amplification of human glyceraldehyde-3-phosphate dehydrogenase was obtained from Stratagene (La Jolla, CA, USA). The polymerase chain reaction (PCR) was repeated for 30 cycles of heating at 94°C for 60 seconds, annealing at 60°C for 30 seconds, and elongation at 72°C for 2 minutes; the PCR products were then separated on a 1.5% agarose gel.

2.4. Immunofluorescence Study and Cytokine Measurement

A multicolor immunofluorescence study was performed with a combination of fluorescein isothiocyanate, phycoerythrin, and phycoerythrin–Cyanine 5 (PC-5). Cells were stained with fluorescently labeled monoclonal antibodies and analyzed by flow cytometry (Epics XL; Beckman Coulter), as described previously [19]. The concentrations of cytokines and chemokines in culture supernatants were determined with a Cytometric Bead Array (CBA) (BD Biosciences, San Diego, CA, USA) according to the manufacturer's instructions.

3. Results

3.1. Differentiation into Monocyte-Macrophage–Lineage Cells of Human BM CD34+ Cells Cultured with a Combination of Cytokines

We first characterized the morphology and surface-antigen expression of human BM CD34+ cells cultured with the

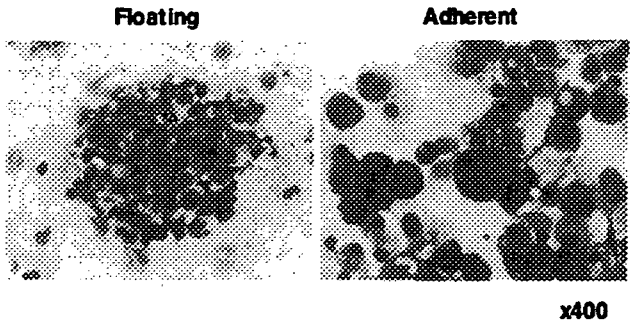

Figure 1. Morphology of monocyte-macrophage cells induced from CD34+ bone marrow (BM) cells in vitro. Human BM CD34+ cells were cultured for 5 weeks in the presence of a cytokine mixture, as described in "Materials and Methods." Floating and adherent cell fractions were subsequently collected separately and cytocentrifuged on a glass slide. Morphology was assessed after Giemsa staining. The experiments were repeated 3 times, and reproducible results were obtained. Representative data are shown (original magnification ×400).

combination of cytokines indicated in "Materials and Methods." During the second week of culture, microscopical observation revealed that a portion of the cells had started to adhere to the bottom of the culture dish. After 3 weeks of cultivation, the cells were clearly divided into floating and adherent fractions. When 1×10^5 CD34+ cells were cultured, approximately 7×10^6 adherent cells and 3×10^6 floating cells were obtained after 5 weeks of cultivation. At the end of the 5-week cultivation period, the floating and adherent fractions were collected separately, and their morphologies were assessed after May-Giemsa staining. As shown in Figure 1, the cells in the floating fraction were small and round and contained little cytoplasm. In contrast, the cells in the adherent fraction were large and contained abundant foamy cytoplasm with protrusions.

We also used flow cytometry to examine the cells for expression of monocyte-macrophage–lineage markers (Figure 2). Most floating cells expressed CD11b, CD31, CD33, and CD97, but no other mature-macrophage markers. The adherent cells, on the other hand, expressed markers of the myelocyte-monocyte lineage, such as CD13, CD14, CD36, CD54, CD64, CD85k, and CD105. It is noteworthy that the adherent cells expressed the mature-macrophage marker CD206, which was not expressed by the peripheral blood monocytes examined as a control (Figure 3).

3.2. Cytokine Secretion by Monocyte-Macrophage–Lineage Cells Induced from Human BM CD34+ Cells

Next, we assessed the cytokine-secreting ability of human BM CD34+ cells cultured with the cytokine combination. At the end of 5 weeks of cultivation, the floating and adherent fractions were collected separately, and cytokine secretion was assessed with the CBA system with and without LPS stimulation. Figure 4 shows that both the floating and adherent cell fractions spontaneously secreted IL-8 and IL-6 without LPS stimulation. After 24 hours of LPS stimulation, IL-6 secretion was enhanced in both fractions, but IL-8 secretion by adherent cells was decreased. TNF-α secretion, on the other hand, was induced in the 2 fractions only after LPS stimulation. It is noteworthy that LPS stimulation induced IL-10 secretion only in the adherent cell fraction and not in the floating cell fraction. Neither IL-1β nor IL-12 secretion was induced by LPS stimulation in either fraction.

We also used reverse transcriptase–polymerase chain reaction analysis to assess the effect of LPS stimulation on the expression levels of cytokine messenger RNA (mRNA). Consistent with the results of the CBA analysis, LPS stimulation enhanced the expression of TNF-α mRNA in both the adherent and floating cell fractions (Figure 5). IL-10 mRNA expression, however, was already detectable in both cell fractions in the unstimulated state, and LPS stimulation did not enhance expression. In addition, LPS stimulation reduced IL-10 mRNA expression in the floating cell fraction. It is interesting that although no secretion of IL-1β protein was detected by the CBA assay, LPS stimulation significantly increased IL-1β mRNA expression in both cell fractions.

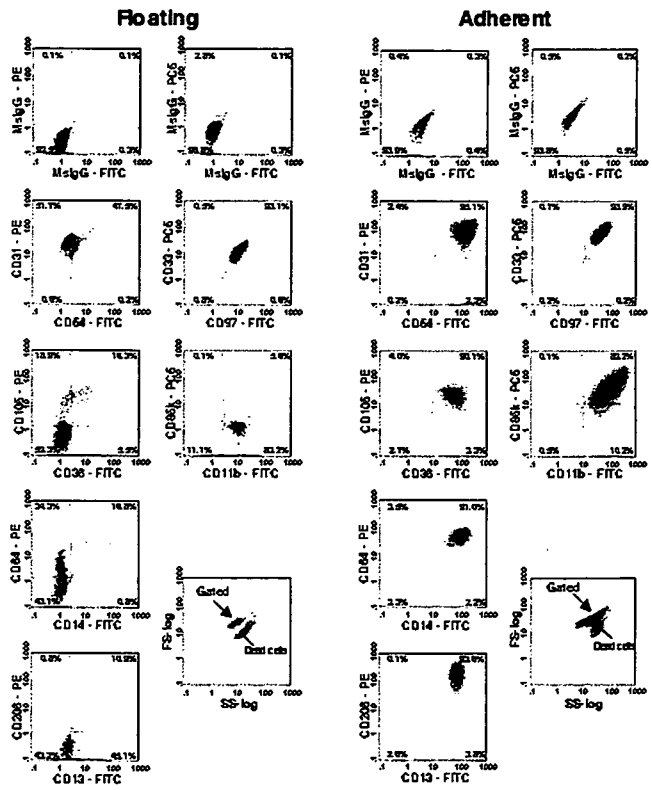

Figure 2. Immunophenotypic analysis of monocyte-macrophage cells induced from CD34+ bone marrow (BM) cells in vitro. Human BM CD34+ cells were cultured for 5 weeks (as in Figure 1). At the end of the culture period, the floating and adherent cell fractions were collected separately, stained with combinations of fluorescently labeled antibodies as indicated, and examined by flow cytometry. The experiments were repeated 3 times, and reproducible results were obtained. Representative histogram data are shown. MsIgG, mouse immunoglobulin G; PE, phycoerythrin; PC-5, PE-Cyanine 5; FITC, fluorescein isothiocyanate; FS, forward light scatter; SS, side light scatter.

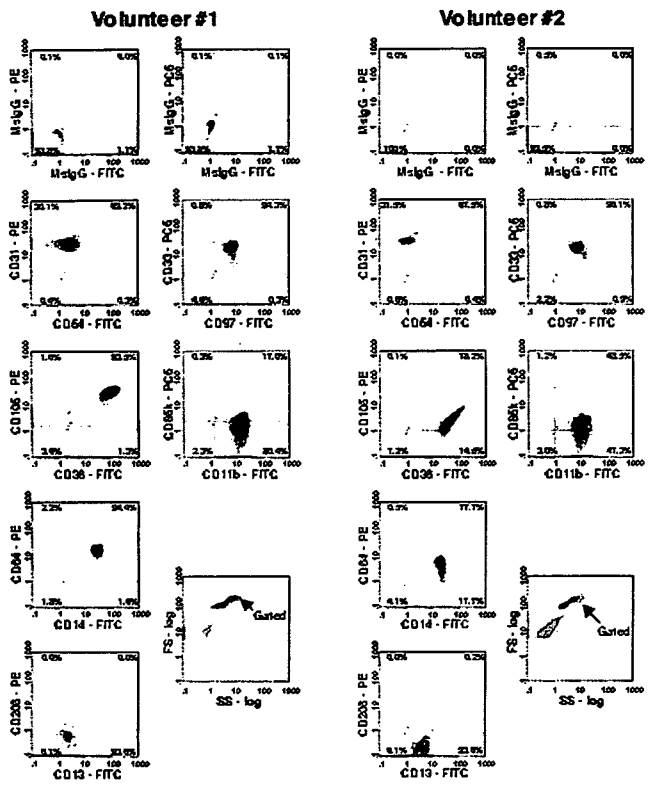

Figure 3. Immunophenotypic analysis of peripheral blood monocytes. Mononuclear cells were obtained from the peripheral blood of healthy volunteers via Ficoll-Paque centrifugation and stained with the indicated combinations of fluorescently labeled antibodies. Monocytes were gated, and the expression of each antigen was analyzed as in Figure 2.

3.3. Effect of G-CSF on TNF-α Secretion by Monocyte-Macrophage–Lineage Cells Induced from Human BM CD34⁺ Cells

As we reported previously, G-CSF directly affects peripheral blood monocytes and reduces LPS-induced TNF-α secretion in a time-dependent manner [20]. We therefore tested the effect of G-CSF on TNF-α secretion by monocyte-macrophage–lineage cells induced from human BM CD34⁺ cells. Because our testing of monocyte-macrophage–lineage cells that had been induced with cytokines and harvested after 5 weeks of cultivation showed that G-CSF did not affect LPS-induced TNF-α secretion (data not shown), we tested cells harvested at different time points. Our assessment of LPS-stimulated cytokine secretion by adherent cells (Figure 6) (but not floating cells; data not shown) collected after 3 weeks of cultivation revealed cytokine-secretion patterns different from those of cells collected after 5 weeks of cultivation. Figure 6 shows that cells cultured for 3 weeks spontaneously secreted low levels of IL-8, but not other cytokines. LPS stimulated the cells to secrete IL-6 and TNF-α and an increased level of IL-8. Pretreatment with G-CSF reduced LPS-induced TNF-α secretion in a time-dependent manner.

4. Discussion

This study has shown that monocyte-macrophage–lineage cells were efficiently induced from CD34⁺ BM cells in liquid culture in the presence of a cocktail of cytokines and that the monocyte-macrophage–lineage cells induced in vitro were capable of cytokine secretion upon stimulation with LPS. Several different subsets of monocyte-macrophage–lineage cells were induced during the course of culture.

For example, 2 distinct fractions, adherent cells and floating cells, were observed at the end of 5 weeks of culture. These 2 fractions were distinctive in both morphology and immunophenotype. Adherent cells were large, had a macrophage-like appearance, and expressed the mature-macrophage markers CD14, CD105, and CD206. In contrast, the floating cells were relatively small and contained little cytoplasm. Only some of them expressed mature-macrophage markers, whereas most

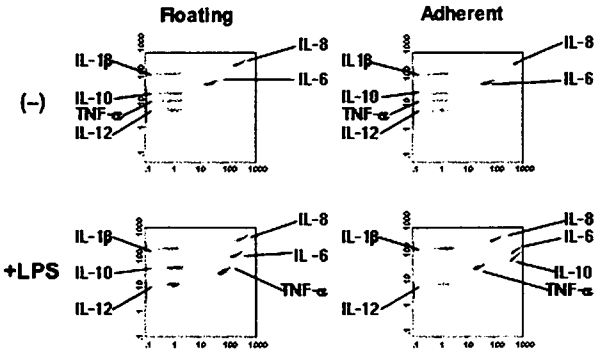

		Floating, ng/mL	Adherent, ng/mL
IL-8	(-)	9.24	26.13
	LPS	12.03	3.90
IL-1 β	(-)	0.07	0.07
	LPS	0.07	0.10
IL-6	(-)	0.87	2.03
	LPS	7.35	20.30
IL-10	(-)	0.02	0.02
	LPS	0.02	34.62
TNF-α	(-)	<0.00	<0.00
	LPS	2.55	0.87
IL12	(-)	<0.00	<0.00
	LPS	<0.00	<0.00

Figure 4. Cytometric Bead Array (CBA) analysis of lipopolysaccharide (LPS)-stimulated cytokine secretion by monocyte-macrophage cells induced from CD34⁺ bone marrow (BM) cells in vitro. Monocyte-macrophage–lineage cells were induced from human BM CD34⁺ cells by cultivation for 5 weeks, as described for Figure 1. At the end of the culture period, the floating and adherent cells were stimulated with and without LPS for 24 hours. Subsequent cytokine secretion was assessed with the CBA system. The histograms obtained (upper panels) and calculated concentrations of each cytokine (table at bottom; <0.00 indicates undetectable) are shown. The experiments were repeated 3 times, and reproducible results were obtained. Representative data are shown. IL-1β indicates interleukin 1β; TNF-α, tumor necrosis factor α.

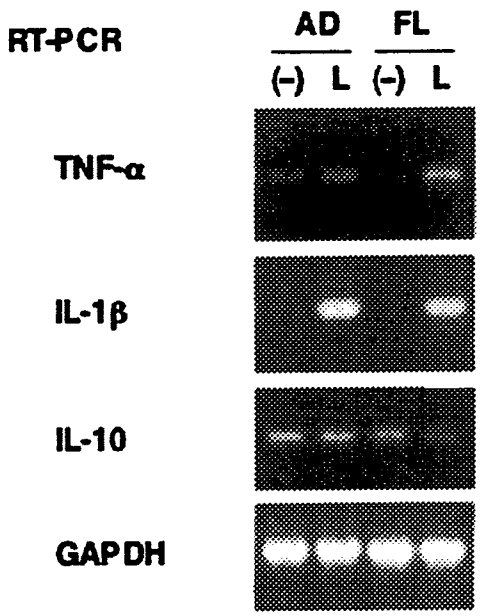

Figure 5. Reverse transcriptase–polymerase chain reaction (RT-PCR) analysis of lipopolysaccharide (LPS)-stimulated cytokine production by monocyte-macrophage cells induced from CD34+ bone marrow (BM) cells in vitro. Monocyte-macrophage–lineage cells were induced from human BM CD34+ cells as described for Figure 1, and then floating (FL) and adherent (AD) cell fractions were collected separately. After stimulation with (L) or without (–) LPS for 24 hours (as described for Figure 4), total RNA was extracted, and the indicated messenger RNA molecules were analyzed by the RT-PCR after complementary DNA synthesis. The experiments were repeated 3 times, and reproducible results were obtained. Representative data are shown. TNF-α indicates tumor necrosis factor α; IL-1β, interleukin 1β; GAPDH, glyceraldehyde-3-phosphate dehydrogenase.

cells expressed myelomonocytic antigens, including CD31, CD33, and CD97. It is interesting that these 2 fractions exhibited different cytokine-secretion abilities. Figure 4 shows that both fractions spontaneously secreted IL-8 and IL-6, and they both secreted TNF-α upon stimulation with LPS. Only the adherent cell fraction secreted IL-10 after LPS stimulation, however. These characteristics suggest that the adherent cell fraction represents mature macrophages, whereas the floating cell fraction may be related to immature monocytes. Evidence that further cultivation of the floating cell fraction induced an adherent cell fraction (data not shown) supports this idea.

It is noteworthy that both cell fractions contained more IL-1β mRNA after LPS stimulation but that no IL-1β secretion at the protein level was detected in either fraction. The data indicate that monocyte-macrophage–lineage cells induced in vitro are capable of producing IL-1β upon stimulation with LPS but that the stimulation is insufficient to induce secretion of IL-1β.

On the other hand, the adherent cells exhibited a profile of cytokine secretion after 3 weeks of cultivation that was distinct from that obtained after 5 weeks. At 3 weeks, the adherent cell fractions displayed almost the same immunophenotype as monocyte-macrophage–lineage cells cultured for 5 weeks; however, the cells spontaneously secreted only low levels of IL-8, and not other cytokines. Although the cells secreted IL-6 and TNF-α after LPS stimulation, they did not secrete IL-10. Thus, our data indicate that different culture conditions induce different monocyte-macrophage–lineage subsets or monocyte-macrophage–lineage cells with different degrees of maturity.

Several studies have shown the induction of monocyte-macrophage–lineage cells by in vitro culture of cells from different cell sources. For example, Akagawa reported that M-CSF–induced monocyte-derived macrophages (M-Mphi) and GM-CSF–induced Mphi (GM-Mphi) differ in morphology, cell surface antigen expression, and function, including Fcγ receptor–mediated phagocytosis, hydrogen peroxide production and sensitivity, catalase activity, susceptibilities to human immunodeficiency virus type 1 and *Mycobacterium tuberculosis*, and suppressor activity [21]. She therefore concluded that the characteristics of GM-Mphi resemble those of human alveolar macrophages. Servet-Delprat et al also

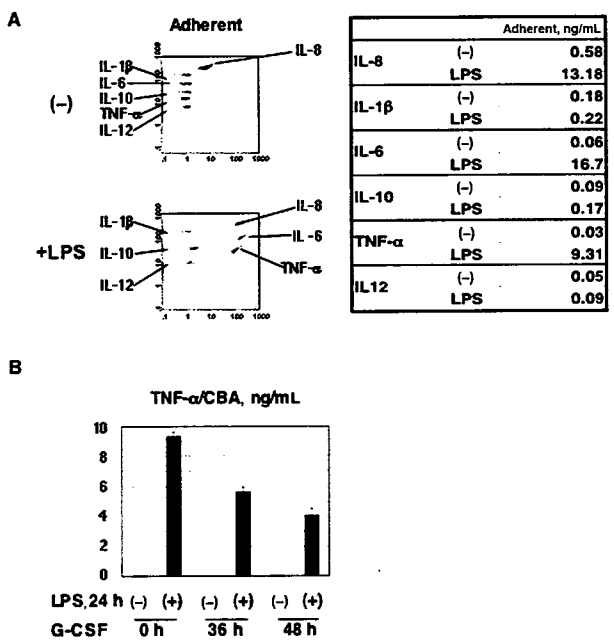

		Adherent, ng/mL
IL-8	(-)	0.58
	LPS	13.18
IL-1β	(-)	0.18
	LPS	0.22
IL-6	(-)	0.06
	LPS	16.7
IL-10	(-)	0.09
	LPS	0.17
TNF-α	(-)	0.03
	LPS	9.31
IL12	(-)	0.05
	LPS	0.09

Figure 6. Effect of granulocyte colony-stimulating factor (G-CSF) on lipopolysaccharide (LPS)-stimulated tumor necrosis factor α (TNF-α) secretion by monocyte-macrophage cells induced from CD34+ bone marrow (BM) cells in vitro. A, Monocyte-macrophage–lineage cells were induced from human BM CD34+ cells after 3 weeks of cultivation in the presence of the mixture of cytokines described in "Materials and Methods." At the end of the culture period, cells were stimulated with LPS for 24 hours. Subsequent cytokine secretion was assessed as in Figure 4. B, Induced monocyte-macrophage cells pretreated and not pretreated with G-CSF were stimulated with (+) and without (–) LPS for 24 hours, and subsequent cytokine secretion was assessed as in (A). The experiment was performed in triplicate, and the data are presented as the mean + SD. The experiments were repeated 3 times, and reproducible results were obtained. Representative data are shown. IL-1β indicates interleukin 1β.

reported that a variety of monocyte-macrophage–lineage cells, including macrophages, osteoclasts, dendritic cells, and microglia, can be induced from murine BM cells by ex vivo culture with different combinations of cytokines [22]. These reports further support our hypothesis that different culture conditions can induce different subsets of monocyte-macrophage–lineage cells.

In conclusion, the results of this study indicate that monocyte-macrophage–lineage cells induced from CD34⁺ BM cells in vitro can be used for functional assays, at least in terms of cytokine secretion. Further investigation is clearly necessary, however; the establishment of culture conditions that enable the induction of different subsets of monocyte-macrophage–lineage cells should provide an ideal experimental model for the analysis of monocyte-macrophage–lineage cell function.

Acknowledgments

This work was supported in part by Health and Labour Sciences Research Grants; a grant for Child Health and Development from the Ministry of Health, Labour and Welfare of Japan; and a grant from the Japan Health Sciences Foundation for Research on Health Sciences Focusing on Drug Innovation, JSPS. This work was supported by KAKENHI 17591131 and 18790751, the Budget for Nuclear Research of the Ministry of Education, Culture, Sports, Science and Technology, based on screening and counseling by the Atomic Energy Commission. This work was also supported by CREST, JST, and a grant from the Charitable Trust Japan Leukemia Research Fund. We thank S. Yamauchi for excellent secretarial work.

References

1. Gordon S. The macrophage. *Bioessays*. 1995;17:977-986.
2. Banchereau J, Steinman RM. Dendritic cells and the control of immunity. *Nature*. 1998;392:245-252.
3. Steinman RM, Turley S, Mellman I, Inaba K. The induction of tolerance by dendritic cells that have captured apoptotic cells. *J Exp Med*. 2000;191:411-416.
4. Teitelbaum SL. Bone resorption by osteoclasts. *Science*. 2000;289: 1504-1508.
5. Perry VH. A revised view of the central nervous system microenvironment and major histocompatibility complex class II antigen presentation. *J Neuroimmunol*. 1998;90:113-121.
6. Elkabes S, DiCicco-Bloom EM, Black IB. Brain microglia/ macrophages express neurotrophins that selectively regulate microglial proliferation and function. *J Neurosci*. 1996;16:2508-2521.
7. Noda M, Nakanishi H, Nabekura J, Akaike N. AMPA-kainate subtypes of glutamate receptor in rat cerebral microglia. *J Neurosci*. 2000;20:251-258.
8. Crofton RW, Diesselhoff-den Dulk MM, van Furth R. The origin, kinetics, and characteristics of the Kupffer cells in the normal steady state. *J Exp Med*. 1978;148:1-17.
9. Thomas ED, Ramberg RE, Sale GE, Sparkes RS, Golde DW. Direct evidence for a bone marrow origin of the alveolar macrophage in man. *Science*. 1976;192:1016-1018.
10. Kennedy DW, Abkowitz JL. Mature monocytic cells enter tissues and engraft. *Proc Natl Acad Sci USA*. 1998;95:14944-14949.
11. Takahashi K, Naito M, Takeya M. Development and heterogeneity of macrophages and their related cells through their differentiation pathways. *Pathol Int*. 1996;46:473-485.
12. Yamamoto T, Naito M, Moriyama H, et al. Repopulation of murine Kupffer cells after intravenous administration of liposome-encapsulated dichloromethylene diphosphonate. *Am J Pathol*. 1996;149: 1271-1286.
13. Wijffels JF, Hendrickx RJ, Steenbergen JJ, Eestermans IL, Beelen RH. Milky spots in the mouse omentum may play an important role in the origin of peritoneal macrophages. *Res Immunol*. 1992; 143:401-409.
14. Lawson LJ, Perry VH, Gordon S. Turnover of resident microglia in the normal adult mouse brain. *Neuroscience*. 1992;48:405-415.
15. Sawano A, Iwai S, Sakurai Y, et al. Flt-1, vascular endothelial growth factor receptor 1, is a novel cell surface marker for the lineage of monocyte-macrophages in humans. *Blood*. 2001;97:785-791.
16. Taghon T, Stolz F, De Smedt M, et al. HOX-A10 regulates hematopoietic lineage commitment: evidence for a monocyte-specific transcription factor. *Blood*. 2002;99:1197-1204.
17. Miyamoto T, Ohneda O, Arai F, et al. Bifurcation of osteoclasts and dendritic cells from common progenitors. *Blood*. 2001;98:2544-2554.
18. Xu MJ, Tsuji K, Ueda T, et al. Stimulation of mouse and human primitive hematopoiesis by murine embryonic aorta-gonad-mesonephros-derived stromal cell lines. *Blood*. 1998;92: 2032-2040.
19. Kiyokawa N, Kokai Y, Ishimoto K, Fujita H, Fujimoto J, Hata JI. Characterization of the common acute lymphoblastic leukaemia antigen (CD10) as an activation molecule on mature human B cells. *Clin Exp Immunol*. 1990;79:322-327.
20. Saito M, Kiyokawa N, Taguchi T, et al. Granulocyte colony-stimulating factor directly affects human monocytes and modulates cytokine secretion. *Exp Hematol*. 2002;30:1115-1123.
21. Akagawa KS. Functional heterogeneity of colony-stimulating factor-induced human monocyte-derived macrophages. *Int J Hematol*. 2002;76:27-34.
22. Servet-Delprat C, Arnaud S, Jurdic P, et al. Flt3⁺ macrophage precursors commit sequentially to osteoclasts, dendritic cells and microglia. *BMC Immunol*. 2002;3:15.

EXPERIMENTAL and MOLECULAR MEDICINE, Vol. 39, No. 2, 170-175, April 2007

Promoter effects of adeno-associated viral vector for transgene expression in the cochlea *in vivo*

Yuhe Liu[1,3], Takashi Okada[2], Tatsuya Nomoto[2], Xiaomei Ke[1], Akihiro Kume[2], Keiya Ozawa[2] and Shuifang Xiao[1]

[1]Department of Otolaryngology
Head and Neck Surgery, Peking University First Hospital
Beijing 100034, China
[2]Division of Genetic Therapeutics
Center for Molecular Medicine
Jichi Medical School
Tochigi 329-0498, Japan
[3]Corresponding author: Tel, 86-10-63078547;
Fax, 86-10-66173427; E-mail, liuyuhe@xinhuanet.com

Accepted 6 February 2007

Abbreviations: AAV, adeno-associated virus; CAG, cytomegalovirus IE enhancer and chicken β-actin promoter; CMV, cytomegalovirus promoter; EF-1α, elongation factor 1 alpha promoter; EGFP, enhanced green fluorescent protein; ITRs, inverted terminal repeats; Myo, myosin 7A promoter; NSE, neuron-specific enolase promoter; RSV, Rous sarcoma virus promoter; WPRE, woodchuck hepatitis; virus posttranscriptional regulatory element

Abstract

The aims of this study were to evaluate the expression of enhanced green fluorescent protein (EGFP) driven by 6 different promoters, including cytomegalovirus IE enhancer and chicken β–actin promoter (CAG), cytomegalovirus promoter (CMV), neuron-specific enolase promoter (NSE), myosin 7A promoter (Myo), elongation factor 1α promoter (EF-1α), and Rous sarcoma virus promoter (RSV), and assess the dose response of CAG promoter to transgene expression in the cochlea. Serotype 1 adeno-associated virus (AAV1) vectors with various constructs were transduced into the cochleae, and the level of EGFP expression was examined. We found the highest EGFP expression in the inner hair cells and other cochlear cells when CAG promoter was used. The CMV and NSE promoter drove the higher EGFP expression, but only a marginal activity was observed in EF-1α promoter driven constructs. RSV promoter failed to drive the EGFP expression. Myo promoter driven EGFP was exclusively expressed in the inner hair cells of the cochlea. When driven by CAG promoter, reporter gene expression was detected in inner hair cells at a dose as low as 3×10^7 genome copies, and continued to increase in a dose-dependent manner. Our data showed that individual promoter has different ability to drive reporter gene expression in the cochlear cells. Our results might provide important information with regard to the role of promoters in regulating transgene expression and for the proper design of vectors for gene expression and gene therapy.

Keywords: cochlea; dependovirus; gene therapy; gene transfer techniques; green fluorescent proteins; promoter regions

Introduction

Gene transfer is a promising tool to study the physiology of the cochlea and cochlear cells. The feasibility of gene therapy in the cochlea has been established (Dazert *et al.*, 2001; Kawamoto *et al.*, 2001; Liu *et al.*, 2005), still, there is a controversy about the transduction of the hair cells or spiral ganglion cell, even when the same vehicle is employed as vectors, such as adenovirus and adeno-associated virus (AAV) (Luebke *et al.*, 2001; Li *et al.*, 2002; Yamasoba *et al.*, 2002; Liu *et al.*, 2005). The previous studies support the hypothesis that this discrepancy may be caused by the differences in delivery methods or driven promoters. It has been shown that individual promoter has distinct ability to express reporter genes in different cell types (Chung *et al.*, 2002; Nomoto *et al.*, 2003; Shevtsova *et al.*, 2005). Tissue or cell specific promoters are capable of restricting gene expression in desirable cells and facilitating persistent or regulated transgene expression (Liu *et al.*, 2004). The cytomegalovirus IE enhancer and chicken β-actin promoter (CAG) drives high level of transgene expression and is one of the most commonly used promoters for gene transfer (Xu *et al.*, 2001). The myosin 7A promoter (Myo) was shown to be the specific promoter of hair cells in the cochlea (Boeda *et al.*, 2001). We have previously demonstrated that, with AAV1 vectors, the CAG promoter can drive transgene expression in the cochlea cells at a highly functional level (Liu *et al.*, 2005). In the present study, we systematically evaluated the promoters CAG, Myo, cytomegalovirus

promoter (CMV), elongation factor 1 alpha promoter (EF-1α), neuron-specific enolase promoter (NSE), and rous sarcoma virus promoter (RSV) for their abilities in gene transfers to the cochlear cells using *in vivo* assays. We also examined the dose-response relationship for CAG promoter over a broad range in the cochlea.

Materials and Methods

Construction and preparation of the proviral plasmids

The AAV1 vector proviral plasmid, pAAV2-*LacZ*, harbors an *Escherichia coli* β-galactosidase expression cassette with the CMV promoter, human growth hormone first intron, and SV40 early polyadenylation sequence; flanked by inverted terminal repeats (ITRs) (Okada *et al.*, 2002). The proviral plasmid pAAV2-CAG-EGFP-WPRE (pAAV2-CAG) consists of enhanced green fluorescent protein (EGFP) gene under the control of the CAG promoter and Woodchuck hepatitis virus posttranscriptional regulatory element (WPRE) and is flanked by ITRs (Liu *et al.*, 2005). *Age*I restriction site was created on 5' end of Myo promoter (Boeda *et al.*, 2001) from C2C12 cell line genomic DNA when subcloned into pCRII-TOPO by PCR (forward primer: 5'-ATGTCGACCT-TGGGCAACCTCTAGACG-3'; reverse primer: 5'-ATC-CGCGGCTTCTACGTCTGCACAC-3'). *Spe*I-*Age*I fragment containing the Myo promoter was subcloned into pAAV2-CAG to obtain pAAV2-Myo-EGFP-WPRE (pAAV2-Myo). PAAV2-CMV-EGFP-WPRE (pAAV2-CMV), pAAV2-EF1α-EGFP-WPRE (pAAV2-EF1α), pAAV2-NSE-EGFP-WPRE (pAAV2-NSE), and pAAV2-RSV-EGFP-WPRE (pAAV2-RSV) were constructed as previously described (Ogasawara *et al.*, 1998; Nomoto *et al.*, 2003; Mochizuki *et al.*, 2004). A schematic illustration of the AAV1 vectors is shown in Figure 1. AAV1-helper plasmid harbors Rep and Cap. Adenovirus helper plasmid pAdeno5 identical to pVAE2AE4-5 encodes the entire E2A and E4 regions, and VA RNA I and II genes (Matsushita *et al.*, 1998). Plasmids were purified with the QIAGEN plasmid purification Kits (QIAGEN K.K., Tokyo, Japan).

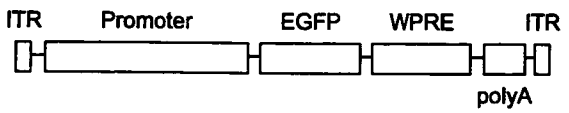

Figure1. Schematic representations of viral vectors constructed. AAV1 vectors were constructed using different promoters to drive reporter gene EGFP and the SV40 polyadenylation sequences (polyA). The promoters in the study include CAG, CMV, NSE, Myo, EF-1α and RSV. The Woodchuck hepatitis virus posttranscriptional regulatory element (WPRE) was inserted 3' of the EGFP cassette in the vectors. ITR, inverted terminal repeats.

Recombinant AAV1 vectors production

Vectors were produced with the AAV1 packaging plasmids pAAV1RepCap and the AAV1 proviral plasmid pAAV2-CAG, pAAV2-Myo, pAAV2-CMV, pAAV2-EF1α, pAAV2-NSE, or pAAV2-RSV. Six kinds of AAV1 vectors were produced using three-plasmid transfection adenovirus-free protocol (Liu *et al.*, 2005). Recombinant AAV1 was harvested at 72 h after transfection by three cycles of freeze/thawing. The crude viral lysate was then purified twice on a cesium chloride (CsCl) two-tier centrifugation gradient as previously described (Okada *et al.*, 2002). The viral stock was titrated by the quantitative real-time PCR of DNase-treated stocks with plasmid standards (Veldwijk *et al.*, 2002). Thus, AAV1 vectors of AAV1-CAG-EGFP-WPRE (AAV1-CAG), AAV1-Myo-EGFP-WPRE (AAV1-Myo), AAV1-CMV-EGFP-WPRE (AAV1-CMV), AAV1-EF1α-EGFP-WPRE (AAV1-EF1α), AAV1-NSE-EGFP-WPRE (AAV1-NSE), and AAV1-RSV-EGFP-WPRE (AAV1-RSV) were constructed. The titers of AAV1 vectors were from 6×10^{12} to 8×10^{13} genome copies (g.c.). For dose-response relationship experiment, vector stocks were serially diluted with artificial perilymph (AP: 145 mM NaCl, 2.7 mM KCl, 2 mM $MgSO_4$, 1.2 mM $CaCl_2$, 5 mM HEPES).

Evaluation of the *in vitro* activity of recombinant AAV1 vectors

To examine the functions of individual promoters, HEK 293 cells were cultured for 36 h, and then transfected with various AAV1 vectors separately (1×10^4 g.c./cell). *Myosin 7A* gene is transcribed in several epithelial cell types that possess microvilli, i.e. renal epithelial cell. Since HEK 293 cell line has been originated from human embryonic kidney epithelial cell, the Myo promoter activity can be assessed in this particular cell line. Forty-eight h after transduction, the cells were recorded for EGFP expression using OLYMPUS IX70 (Olympus corporation, Tokyo, Japan) fluorescence microscope. Cells with green fluorescence were considered "positive" for transgene expression.

Surgical procedures and cochlear perfusions

All animal studies were approved by the ethics committee of Jichi Medical School in Japan and Peking University First Hospital in China. They were performed following the animal research guidelines at Jichi Medical School and Peking University First

Hospital. Seventy female C57BL/6J mice (4 weeks old, CLEA Japan, Tokyo, Japan) and 30 male Sprague-Dawley rats (5 weeks old, CLEA Japan, Tokyo, Japan) with normal Preyer's reflexes were included in this study. Surgical procedures and cochlear perfusion of the animals were performed as previously described (Liu *et al.*, 2005). In the testing groups, 5 μl of AAV1 vectors solution was microinjected into the unilateral cochlea. Five mice received control cochlear perfusions with artificial perilymph only. Each AAV1 vector was injected into 5 animals with 3 $\times 10^{10}$ g.c./cochlea. Injected dose of AAV1-CAG vector into 5 mice was varied from 3 $\times 10^{10}$ to 3 $\times$ 10^{7} g.c./cochlea for dose response study.

Histological study

The capability of the transgene expression in the cochlear cells for various AAV1 vectors was determined by visualizing EGFP levels. The animals were sacrificed 2 weeks after injection, and the cochleae were harvested and the stapes footplates were removed. After fixing and decalcifying, the cochleae were made by cryosection (10 μm). The EGFP expression was detected under OLYMPUS IX70 fluorescence microscope using a standard fluoresce in isothiocyanate (FITC) filter set and a Studio Lite software (Olympus corporation, Tokyo, Japan). Level of expression was graded by fluorescent intensity.

Results

Evaluation of activity of all promoters *in vitro*

The EGFP expression in the HEK 293 cell was detected with any of the AAV1 vectors, indicating that all promoters were functional. However, their expression levels were different (Figure 2). Robust EGFP expression with CAG promoter was shown in the HEK 293 cell, followed by CMV, NSE, EF-1α and RSV. Myo promoter was just weak in 293 cells.

EGFP expression profile within the cochlea under different promoter

The pattern of EGFP expression in the cochlear cells was quite similar in both mice and rat for each promoter. Distribution of AAV1 vector-mediated EGFP expression was examined throughout the cochlea for all promoters tested (Table 1). With CAG promoter, a robust EGFP expression was identified in the various cochlear cells, including the inner hair cells, spiral ganglion cells, inner sulcus cells, Hensen's cells and mesenchymal cells (Figure 3B). A

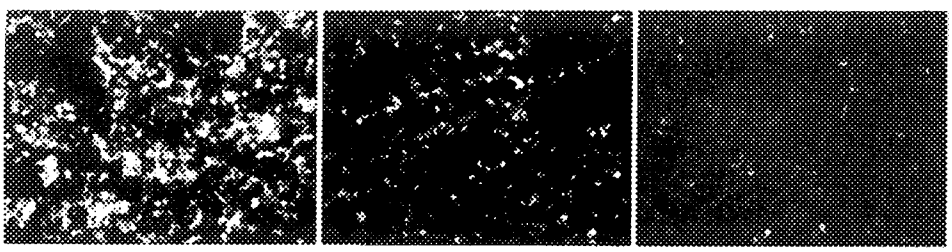

Figure 2. EGFP expression in the HEK293 cell transduced with AAV1 vectors harboring distinct promoters. Robust EGFP expression with CAG promoter was shown, EGFP expression with CMV is similar to that with CAG, and EGFP expression with NSE to with RSV and EF-1α. Myo promoter was just weak in 293 cells.

Table 1. Transgene expression with distinct promoter in the cochlear cells

Promoter	Inner hair cells	Outer hair cells	Spiral ganglion cells	Stria vascularis cells	Spiral ligament cells	Reissner's membrane	Inner sulcus cells	Claudius' cells	Mesenchymal cells
CAG	+	-	+	-	+	+	+	-	+
CMV	+	-	+	-	+	+	+	-	+
NSE	-	-	+	-	+	+	-	-	+
EF-1α	-	-	+	-	+	-	-	-	+
Myo	+	-	-	-	-	-	-	-	-
RSV	-	-	-	-	-	-	-	-	-

+ means EGFP expression in the cells, while - means no fluorescence in the cells.

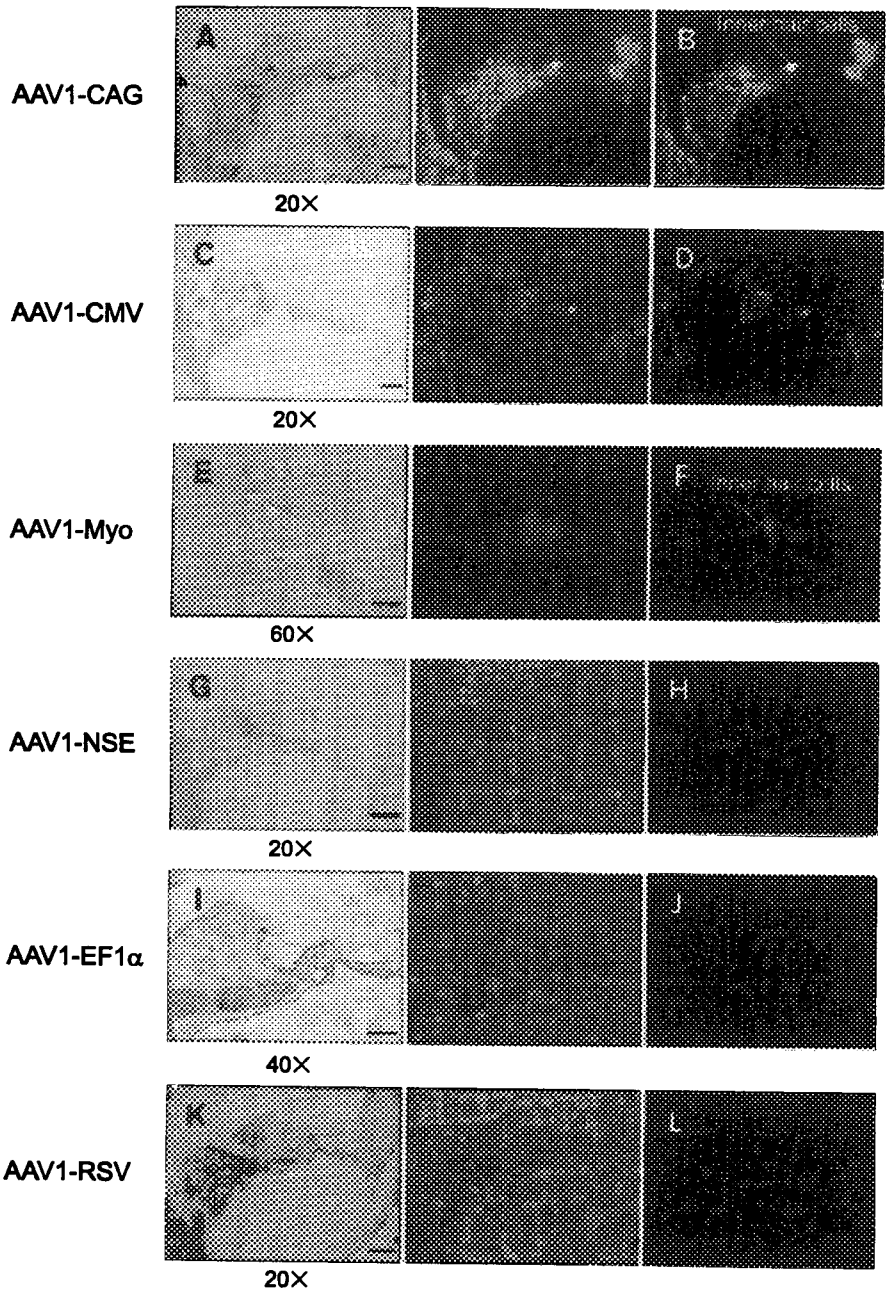

Figure 3. Transduction of cochlear radical cryosection with AAV1 vectors harboring distinct promoters showing EGFP expression in the cochlear various cells. Light photomicrograph of cochlear cryosection is shown in (A,C,E,G,I,K). The fluorescence photomicrograph (green fluorescence from transgene) of the cryosection is shown in (B,D,F,H,J,L). Scale bar, 20×: 50; 40×: 25; 60×: 25 μm separately.

similar transgene expression pattern (Figure 3D) was also observed when AAV1-CMV vector was used. In contrast, the EGFP expression under NSE and EF- 1α promoters was present in all kinds but the inner hair cells of cochlear cells (Figure 3H and J). As reported previously (Boeda *et al.*, 2001), Myo promoter driven EGFP was exclusively expressed in the inner hair cells of cochlea (Figure 3F), while EGFP expression in the cochlear cells was rarely observed with the RSV promoter (Figure 3L). Consistent with the previous findings (Liu *et al.*, 2005), no EGFP expression was detected in the outer hair cells, supporting pillar cells, or the stria vascularis cells with all tested promoters. The level of EGFP expression in the cochlear cells was highest with CAG promoter, followed by CMV promoter. NSE promoter only drove weak expression of EGFP, while EF-1α promoter displayed the least activity.

Our results indicate that, among these promoters, CAG promoter was the most efficient in transducing the cochlear cells.

Dose-response relationship for AAV1-CAG vector

Within the dose-effect groups with AAV1-CAG, a significant effect of dosage on the number of EGFP-expressing cochlear cells was found by one-way ANOVA ($P < 0.001$). CAG promoter driven EGFP expression in inner hair cells was detected at a dose as low as 3×10^7 genome copies, with expression increasing in a dose-dependent manner.

Discussion

The various factors affecting the transcription of a transgene includes the promoter containing 5'flanking region, 3'UTR, enhancer, suppressor, insulator sequences and the type and activity of transcription factors available in the transfected cells. This study showed that all 6 promoters, including viral, mammalian cells promoters, were capable of driving EGFP expression in HEK 293 cells, suggesting that the HEK 293 cell possesses all essential transcription factors for recognizing the diverse promoter sequences applied in this study. The CAG promoter appeared to be more efficient than other promoters based on the following observations: (1) more cells transduced in an equal dose comparison; (2) greater spreads of EGFP-expressing cell groups; and (3) CAG promoter-driven expression in more cell types, especially the inner hair cells, which were rarely found with other promoters except for CMV promoter. These results extend our knowledge about the promoter-related characteristics of AAV1-mediated gene transfer in the cochlea.

Interestingly, our data demonstrate that, in comparison with NSE, EF-1α and RSV promoters, CAG, CMV and hair cells specific promoter-Myo can drive EGFP expression in the inner hair cells. Even though certain promoters, such as EF-1α and RSV promoters, showed robust activity in many tissues, their activities are limited in the cochlear cells. Nowadays, it still has not been known why NSE, EF-1α and RSV promoters are inactive in the inner hair cells. One likely explanation is that inner hair cells may not express some transcription factors, which were necessary for these promoters to be actived. On the other hand, the inner hair cells may have all necessary components for the full transcriptional activity of the CAG, CMV or Myo promoters. Another possibility is transcriptional shutdown or promoter silencing in the inner hair cells. These phenomena have been observed previously in different organs such as the liver, lungs, and muscles (Hartikka *et al.*, 1996; Chen *et al.*, 2001; Gill *et al.*, 2001). Besides the known mechanisms for promoter silencing, such as DNA methylation, it has been demonstrated that the inclusion of EBN1 and OriP sequences into vector constructs may delay the process of promoter silencing (Al-Dosari *et al.*, 2006). Those elements also have been known to play an important role during viral infection in retention, replication, nuclear localization, binding to the nuclear matrix of the target cell, and tran-scriptional up-regulation (Cui *et al.*, 2001). Nevertheless, the mechanism of promoter inactivation remains to be poorly understood. The development of the vectors, which was capable of expressing high levels of transgene products, remains as an occasional finding. A thorough investigation on the mechanisms underlying episomal gene expression would be important for successful development of gene therapy.

Dose-dependent response for AAV gene transfer in other tissue has been previously reported (Klein *et al.*, 2002), and the wide range of doses has established minimal doses for transgene expression (10^7 particles). There is a shift toward lower potency for bicistronic vectors. The present study determined the dose dependency and minimum effective doses for AAV1 gene transfer using CAG promoter for the cochlear cells.

The direct measurement of transgene expression level in individual cells of cochlea *in vivo* is an important evaluation for cochlear gene therapy. Nevertheless, quantifying the number of cells transduced remains an important additional issue and a combination of protein expression and cell transduction efficiency may permit us to estimate the amount of gene product per cell under appropriate conditions. The gene transduction of the cochlear inner hair cells requires efficient promoter systems, which ensure potent and stable expression of exogenous genes. In this study, we demonstrated that the CAG and CMV promoters showed stable and efficient activity in the cochlear cells, the Myo promoter was specific for gene transfer in the inner hair cells. The stable and efficient promoter activities might be necessary for cochlear gene therapy strategies. From the data obtained by this study, it might be able to extend our knowledge both in the basic and clinical gene research fields.

Acknowledgement

This study was supported in part by Research Grants from the Ministry of Education, Culture, Sports, Science and Technology, the Ministry of Health, Labor and Welfare, and the Vehicle Racing Commemorative Foundation.

References

Al-Dosari M, Zhang G, Knapp JE, Liu D. Evaluation of viral and mammalian promoters for driving transgene expression in mouse liver. Biochem Biophys Res Commun 2006;339:673-8

Boeda B, Weil D, Petit C. A specific promoter of the sensory cells of the inner ear defined by transgenesis. Hum Mol Genet 2001;10:1581-9

Chen ZY, Yant SR, He CY, Meuse L, Shen S, Kay MA. Linear DNAs concatemerize *in vivo* and result in sustained transgene expression in mouse liver. Mol Ther 2001;3:403-10

Chung S, Andersson T, Sonntag KC, Bjorklund L, Isacson O, Kim KS. Analysis of different promoter systems for efficient transgene expression in mouse embryonic stem cell lines. Stem Cells 2002;20:139-45

Cui FD, Kishida T, Ohashi S, Asada H, Yasutomi K, Satoh E, Kubo T, Fushiki S, Imanishi J, Mazda O. Highly efficient gene transfer into murine liver achieved by intravenous administration of naked Epstein-Barr virus (EBV)-based plasmid vectors. Gene Ther 2001;8:1508-13

Dazert S, Aletsee C, Brors D, Gravel C, Sendtner M, Ryan A. *In vivo* adenoviral transduction of the neonatal rat cochlea and middle ear. Hear Res 2001;151:30-40

Gill DR, Smyth SE, Goddard CA, Pringle IA, Higgins CF, Colledge WH, Hyde SC. Increased persistence of lung gene expression using plasmids containing the ubiquitin C or elongation factor 1alpha promoter. Gene Ther 2001;8:1539-46

Hartikka J, Sawdey M, Cornefert-Jensen F, Margalith M, Barnhart K, Nolasco M, Vahlsing HL, Meek J, Marquet M, Hobart P, Norman J, Manthorpe M. An improved plasmid DNA expression vector for direct injection into skeletal muscle. Hum Gene Ther 1996;7:1205-17

Kawamoto K, Oh SH, Kanzaki S, Brown N, Raphael Y. The functional and structural outcome of inner ear gene transfer via the vestibular and cochlear fluids in mice. Mol Ther 2001;4:575-85

Klein RL, Hamby ME, Gong Y, Hirko AC, Wang S, Hughes JA, King MA, Meyer EM. Dose and promoter effects of adeno-associated viral vector for green fluorescent protein expression in the rat brain. Exp Neurol 2002;176: 66-74

Li Duan M, Bordet T, Mezzina M, Kahn A, Ulfendahl M. Adenoviral and adeno-associated viral vector mediated gene transfer in the guinea pig cochlea. Neuroreport 2002;13: 1295-9

Liu BH, Wang X, Ma YX, Wang S. CMV enhancer/human PDGF-beta promoter for neuron-specific transgene expression. Gene Ther 2004;11:52-60

Liu Y, Okada T, Sheykholeslami K, Shimazaki K, Nomoto T, Muramatsu SI, Kanazawa T, Takeuchi K, Ajalli R, Mizukami H, Kume A, Ichimura K, Ozawa K. Specific and efficient transduction of cochlear inner hair cells with recombinant adeno-associated virus type 3 vector. Mol Ther 2005;12:725-733

Luebke AE, Foster PK, Muller CD, Peel AL. Cochlear function and transgene expression in the guinea pig cochlea, using adenovirus- and adeno-associated virus-directed gene transfer. Hum Gene Ther 2001;12:773-81

Matsushita T, Elliger S, Elliger C, Podsakoff G, Villarreal L, Kurtzman GJ, Iwaki Y, Colosi P. Adeno-associated virus vectors can be efficiently produced without helper virus. Gene Ther 1998;5:938-45

Mochizuki S, Mizukami H, Kume A, Muramatsu S, Takeuchi K, Matsushita T, Okada T, Kobayashi E, Hoshika A, Ozawa K. Adeno-associated virus (AAV) vector-mediated liver- and muscle-directed transgene expression using various kinds of promoters and serotypes. Gene ther Mol Biol 2004;8:9-18

Nomoto T, Okada T, Shimazaki K, Mizukami H, Matsushita T, Hanazono Y, Kume A, Katsura K, Katayama Y, Ozawa K. Distinct patterns of gene transfer to gerbil hippocampus with recombinant adeno-associated virus type 2 and 5. Neurosci Lett 2003;340:153-7

Ogasawara Y, Urabe M, Ozawa K. The use of heterologous promoters for adeno-associated virus (AAV) protein expression in AAV vector production. Microbiol Immunol 1998;42:177-85

Okada T, Nomoto T, Shimazaki K, Lijun W, Lu Y, Matsushita T, Mizukami H, Urabe M, Hanazono Y, Kume A, Muramatsu S, Nakano I, Ozawa K. Adeno-associated virus vectors for gene transfer to the brain. Methods 2002;28:237-47

Shevtsova Z, Malik JM, Michel U, Bahr M, Kugler S. Promoters and serotypes: targeting of adeno-associated virus vectors for gene transfer in the rat central nervous system *in vitro* and *in vivo*. Exp Physiol 2005;90:53-9

Veldwijk MR, Topaly J, Laufs S, Hengge UR, Wenz F, Zeller WJ, Fruehauf S. Development and optimization of a real-time quantitative PCR-based method for the titration of AAV-2 vector stocks. Mol Ther 2002;6:272-8

Xu L, Daly T, Gao C, Flotte TR, Song S, Byrne BJ, Sands MS, Parker Ponder K. CMV-beta-actin promoter directs higher expression from an adeno-associated viral vector in the liver than the cytomegalovirus or elongation factor 1 alpha promoter and results in therapeutic levels of human factor X in mice. Hum Gene Ther 2001;12:563-73

Yamasoba T, Suzuki M, Kondo K. Transgene expression in mature guinea pig cochlear cells *in vitro*. Neurosci Lett 2002;335:13-6

THE JOURNAL OF BIOLOGICAL CHEMISTRY VOL. 282, NO. 36, pp. 26369–26380, September 7, 2007

Soluble ST2 Blocks Interleukin-33 Signaling in Allergic Airway Inflammation*[S]

Received for publication, June 14, 2007, and in revised form, June 29, 2007 Published, JBC Papers in Press, July 10, 2007, DOI 10.1074/jbc.M704916200

Hiroko Hayakawa[‡], Morisada Hayakawa[‡1], Akihiro Kume[§], and Shin-ichi Tominaga[‡]

From the [‡]Department of Biochemistry and [§]Division of Genetic Therapeutics, Jichi Medical University, 3311-1 Yakushiji, Shimotsuke-shi, Tochigi 329-0498, Japan

The ST2 gene produces a soluble secreted form and a transmembrane form, referred to as soluble ST2 and ST2L, respectively. A recent study has reported that interleukin (IL)-33 is a specific ligand of ST2L and induces production of T helper type 2 (Th2) cytokines. Although soluble ST2 is highly produced in sera of asthmatic patients and plays a critical role for production of Th2 cytokines, the function of soluble ST2 in relation to IL-33 signaling remains unclear. Here we show antagonistic effects of soluble ST2 on IL-33 signaling using a murine thymoma EL-4 cells stably expressing ST2L and a murine model of asthma. Soluble ST2 directly bound to IL-33 and suppressed activation of NF-κB in EL-4 cells stably expressing ST2L, suggesting that the complex of soluble ST2 and IL-33 fails to bind to ST2L. In a murine model of asthma, pretreatment with soluble ST2 reduced production of IL-4, IL-5, and IL-13 from IL-33-stimulated splenocytes. These results indicate that soluble ST2 acts as a negative regulator of Th2 cytokine production by the IL-33 signaling. Our study provides a molecular mechanism wherein soluble ST2 modulates the biological activity of IL-33 in allergic airway inflammation.

The interleukin (IL)-1[2] receptor family plays important roles in inflammatory and immunological responses. The ST2 gene is a member of the IL-1 receptor family, producing a soluble secreted form and a transmembrane form, soluble ST2 and ST2L, respectively (1–3). These proteins are generated by alternative splicing of pre-mRNA. The structure of ST2L is similar to that of IL-1 receptor type I (IL-1RI), consisting of three extracellular immunoglobulin domains and an intracellular Toll-interleukin-1 receptor domain. Although the extracellular domain is common to soluble ST2 and ST2L, soluble ST2 lacks the transmembrane and intracellular Toll-interleukin-1 receptor domains. The ST2 gene is expressed in several cells including fibroblasts and mast cells (1, 4). In particular, ST2L is preferentially expressed in murine and human Th2 cells and can be utilized as a specific marker of Th2 cells in *in vitro* experiments (5–8). Therefore, the function of ST2L has been suggested to correlate with Th2 cell-mediated immunological responses. However, ST2L has been an orphan receptor ever since it was first reported (5). Late in 2005, IL-33, a newly discovered member of the IL-1 cytokine family, was finally reported as a specific ligand for ST2L (9).

The IL-33 gene, also described as a nuclear factor expressed in high endothelial venules (NF-HEV) (10), codes a 31-kDa protein that does not contain a signal sequence for secretion, similar to the IL-1α, IL-1β, and IL-18 genes (11, 12). Previous study has demonstrated the processing and function of the IL-33 protein (9). The precursor 31-kDa protein (pre-IL-33) was cleaved by caspase-1 into a mature 18-kDa protein (IL-33) in *in vitro* experiments using a recombinant protein. Functional analysis has shown that IL-33 bound to murine mast cells expressing ST2L and stimulated the intracellular signaling pathway, leading to the activation of NF-κB and mitogen-activated protein kinases. In addition, the production of Th2 cytokines and severe pathological changes in mucosal organs were induced by administration of IL-33 to mice. Previous studies before the discovery of IL-33 had already shown that ST2L is associated with the production of Th2 cytokines. Levels of Th2 cytokines were decreased in asthmatic mice by administration of the antibody that blocks ST2L and in a pulmonary granuloma model using mice lacking the ST2 gene (7, 13). Therefore, these results suggest that IL-33 signaling via ST2L plays important roles in Th2 cell-mediated immunological responses including the production of Th2 cytokines.

On the other hand, previous studies in human patients and animal models have shown that the level of soluble ST2 in sera was elevated in asthmatic disease (14, 15). Therefore, it has been suggested that soluble ST2 may also play a critical role in Th2 cell-mediated diseases. In fact, administration of a recombinant soluble ST2-Fc fusion protein or a soluble ST2 expression vector to asthmatic mice effectively attenuated inflammatory responses and production of Th2 cytokines (7, 15). These results of therapeutic experiments indicate that soluble ST2 negatively regulates the Th2 cell-mediated immunological responses, in opposition to ST2L. However, the molecular mechanism of negative regulation by soluble ST2 remains unclear. In addition, it has not been addressed whether soluble ST2 is associated with IL-33 signaling.

In this study, using a murine thymoma cell line, EL-4, stably expressing ST2L and a murine model of asthma, we demonstrated that soluble ST2 had a negative function in IL-33 signal-

* This work was supported by a Grant-in-Aid from the Ministry of Education, Culture, Sports, Science and Technology of Japan. The costs of publication of this article were defrayed in part by the payment of page charges. This article must therefore be hereby marked "*advertisement*" in accordance with 18 U.S.C. Section 1734 solely to indicate this fact.

[S] The on-line version of this article (available at http://www.jbc.org) contains supplemental Figs. S1 and S2.

[1] To whom correspondence should be addressed. Tel.: 81-285-58-7324; Fax: 81-285-44-2158; E-mail: morisada@jichi.ac.jp.

[2] The abbreviations used are: IL, interleukin; Th, T helper; IFN-γ, interferon-γ; OVA, ovalbumin; NF-κB, nuclear factor-κB; IκB, inhibitor of NF-κB; PBS, phosphate-buffered saline; FITC, fluorescein isothiocyanate; RPE, R-phycoerythrin; EMSA, electrophoretic mobility shift assay; ELISA, enzyme-linked immunosorbent assay; SAL, saline.

ing. Binding and functional analyses showed that soluble ST2 inhibited the binding of IL-33 to ST2L-positive cells and that the activation of NF-κB and the production of Th2 cytokines in the IL-33 signaling were suppressed in the presence of soluble ST2. Our data suggest that soluble ST2 negatively modulates the production of Th2 cytokines through IL-33 signaling in allergic airway inflammation.

EXPERIMENTAL PROCEDURES

Animals—Male and female BALB/c mice, 7–8 weeks of age, were purchased from Japan SLC, Inc. (Shizuoka, Japan). All of the mice were housed in an animal research facility of the Jichi Medical University under pathogen-free conditions. All of the experimental procedures were approved by the Animal Research Ethics Board of Jichi Medical University.

Sensitization and Aeroallergen Challenge—The mice were sensitized by intraperitoneal injection with 100 μg of ovalbumin (OVA) (Sigma-Aldrich) and 20 mg of aluminum potassium sulfate (Sigma-Aldrich) in saline or 20 mg of aluminum potassium sulfate alone in saline on days 0 and 7. On days 14 and 15, the mice were challenged twice daily at intervals of 4 h with 1% (w/v) OVA in saline or saline alone for 30 min using an ultrasonic nebulizer (Omron Corp., Tokyo, Japan) (15). The mice were sacrificed 3–48 h after the last aeroallergen challenge, and sera and tissues were obtained for further analyses. Briefly, blood was drawn from the caudal vena cava and left for 30 min, and then the serum was separated by centrifugation. The sera were stored at −80 °C until assay.

Cell Culture—Human embryonic kidney HEK293T cells were cultured in Dulbecco's modified Eagle's medium (Sigma-Aldrich) supplemented with 10% fetal bovine serum (Thermo Electron, Melbourne, Australia). Murine thymoma EL-4 cells were cultured in RPMI 1640 medium (Sigma-Aldrich) supplemented with 5% fetal bovine serum (Sigma-Aldrich) and 50 μM 2-mercaptoethanol (RPMI 1640 growth medium).

Reverse Transcription-PCR Analysis—Total RNAs were isolated from murine tissues using TRI reagent (Sigma-Aldrich). The total RNA was treated with RNase-free DNase I; then first-strand cDNA was synthesized as described previously (16). PCR amplification was performed using 0.5 units of AmpliTaq Gold DNA polymerase (Applied Biosystems, Foster, CA), 0.5 μM each of the forward and reverse primers, and the first-strand cDNAs derived from 0.25 μg of DNase I-treated RNA. After cDNAs were treated at 94 °C for 10 min, PCR was carried out for 25 (β-actin), 28 (IL-33), or 33 (ST2 and ST2L) cycles at 94 °C for 1 min, 60 °C for 1 min, and 72 °C for 1.5 min, followed by treatment at 72 °C for 10 min. The nucleotide sequences of primers used were as follows: ST2, forward 5′-TGGCATGATAAGGCACACCATAAGGCT-3′ and reverse 5′-GTTAGTGTCTCTCTCCCTCCCATGC-3′; ST2L, forward 5′-TGCGTACATCATTTACCCTCGGGTC-3′ and reverse 5′-TCTTGTGCCACAAGAGTGAAGTAGG-3′; IL-33, forward 5′-ATGAGACCTAGAATGAAGTATTCCA-3′ and reverse 5′-TTAGATTTTCGAGAGCTTAAACATA-3′; and β-actin, forward 5′-ATCTACGAGGGCTATGCTCT-3′ and reverse 5′-TACTCCTGCTTGCTGATCCA-3′. Seven microliters of PCR products were developed by electrophoresis on 2% agarose gels, and then the gels were stained with ethidium bromide. The intensity of DNA bands was quantified using the public domain NIH Image program (developed at the United States National Institutes of Health). The size of PCR products was as follows: ST2 (754 bp), ST2L (739 bp), IL-33 (801 bp), and β-actin (576 bp).

Construction of Plasmids—Constructions of pET-21-mIL-33 and pET-21-mIL-1β proceeded as follows. The coding regions of mature IL-33 and IL-1β proteins were obtained from cDNA derived from spleens of BALB/c mice by PCR amplification. The nucleotide sequences of primers containing an EcoRI or an XhoI site were as follows: IL-33, forward 5′-GAATTCACATTGAGCATCCAAGGAAC-3′ and reverse 5′-CTCGAGGATTTTCGAGAGCTTAAACA-3′; IL-1β, forward 5′-GAATTCGTTCCCATTAGACAGCTGCA-3′ and reverse 5′-CTCGAGGGAAGACACAGATTCCATGG-3′. PCR products were digested with EcoRI and XhoI and then ligated into an EcoRI/XhoI-digested pET-21a (+) vector (Novagen, Madison, WI). Expression vectors of murine soluble ST2 were constructed using pEF6-V5-His (Invitrogen) and pEF6-FLAG-His. Construction of pEF6-FLAG-His proceeded as follows. A fragment containing FLAG and His tags (FLAG-His) was created by annealing a sense oligonucleotide (5′-GCGGCCGCTGACTACAAGGATGACGATGACAAGCGTACCGGTC-3′) and an antisense oligonucleotide (5′-GTTTAAACTCAATGGTGATGGTGATGATGACCGGTACGCTTGT-3′), and the annealed fragment was elongated and subcloned into a pCR2.1 TOPO (Invitrogen). A NotI/PmeI-digested FLAG-His fragment was ligated into a NotI/PmeI-digested pEF6-V5-His. Murine ST2 (mST2) cDNA was amplified from pEF-BOS-mST2 (17) by PCR using a forward primer containing a KpnI site (5′-GGTACCATGATTGACAGACAGAGAAT-3′) and a reverse primer containing a NotI site (5′-GCGGCCGCAGCAATGTGTGAGGGACACT-3′). A KpnI/NotI-digested PCR product was ligated into a KpnI/NotI-digested pEF6-V5-His and pEF6-FLAG-His to obtain final products pEF6-mST2-V5-His and pEF6-mST2-FLAG-His, respectively. Constructions of pEF6-mST2L-FLAG and pEF6-mIL-1RI-FLAG proceeded as follows. Murine ST2L (mST2L) cDNA was amplified from pEF-BOS-mST2L (5) by PCR using a forward primer containing a BamHI site (5′-GGATCCATGATTGACAGACAGAGA-3′) and a reverse primer containing a NdeI site (5′-CATATGAAAGTGTTTCAGGTCTAA-3′). The PCR product was subcloned into a pCR2.1 TOPO (pCR2.1-mST2L). A FLAG fragment containing a stop codon was created by annealing FLAG-s (5′-TATGGATTACAAGGATGACGACGATAAGTAGA-3′) and FLAG-as (5′-CTAGTCTACTTATCGTCGTCATCCTTGTAATCCA-3′), and the annealed fragment was ligated into a NdeI/SpeI-digested pCR2.1-mST2L. Finally, the mST2L-FLAG fragment was digested with BamHI and SpeI and ligated into a BamHI/SpeI-digested pEF6/V5-His. Murine IL-1RI (mIL-1RI) cDNA was obtained from cDNA derived from EL-4 cells by PCR amplification using primers containing a KpnI or a NdeI site (forward 5′-GGTACCATGGAGAATATGAAAGTGCTA-3′ and reverse 5′-CATATGGCCGAGTGGTAAGTGTGTTGC-3′). Murine ST2L cDNA in pEF6-mST2L-FLAG was replaced with mIL-1RI cDNA, using KpnI and NdeI digestion. All of the constructs were confirmed to be correct by DNA sequencing analysis.

Purification of Recombinant IL-33 and IL-1β Proteins—Recombinant murine IL-33 and IL-1β proteins containing a T7 tag at the N terminus and a His tag at the C terminus (rIL-33 and rIL-1β) were produced in bacteria. BL-21 Codon-Plus (DE3)-RIL (Stratagene, La Jolla, CA) was transformed with pET-21-mIL-33 or pET-21-mIL-1β. The bacteria were cultured at 37 °C until the A_{600} reached 0.6; then expression of recombinant protein was induced by the addition of isopropyl β-D-thiogalactopyranoside to a final concentration of 1 mM. Three hours after culture at 25 °C, the bacteria were harvested, and the pellets were resuspended in lysis buffer (50 mM Na_2HPO_4, 300 mM NaCl, 10 mM imidazole) containing 1 mg/ml lysozyme. After sonication, the soluble cytoplasmic fraction was isolated by centrifugation. The fraction was loaded onto a nickel-nitrilotriacetic acid-agarose (Qiagen) column. The proteins were eluted with elution buffer (50 mM Na_2HPO_4, 300 mM NaCl, 250 mM imidazole). After dialysis against T7 tag binding buffer (4.3 mM Na_2HPO_4, 1.5 mM KH_2PO_4, 2.7 mM KCl, 137 mM NaCl, 0.1% (v/v) Tween 20, pH 7.3), the proteins were purified using a T7 tag affinity purification kit (Novagen). The proteins were eluted from the column with 0.1 M citric acid (pH 2.2) and neutralized with 2 M Tris base (pH 10.4). After desalting and concentrating the protein using Centricon YM-3 (Millipore, Bedford, MA), the purified proteins were dialyzed against PBS (8 mM Na_2HPO_4, 1.5 mM KH_2PO_4, 2.7 mM KCl, 137 mM NaCl). The protein concentration was determined by the Bradford method using protein assay dye reagent (Bio-Rad) with calibration using bovine serum albumin (Sigma-Aldrich). The protein purity was evaluated using a silver staining kit (Daiichi Pure Chemicals, Tokyo, Japan).

Purification of Recombinant Soluble ST2 Proteins—Recombinant soluble ST2 proteins containing V5-His or FLAG-His tags at the C terminus (ST2-V5 and ST2-FLAG) were purified as described previously (18). Briefly, HEK293T cells were transiently transfected with pEF6-mST2-V5-His or pEF6-mST2-FLAG-His using the calcium-phosphate method. Sixteen hours after transfection, the cells were cultured in serum-free Dulbecco's modified Eagle's medium for 48 h. The secreted recombinant proteins in the culture supernatant were purified by affinity chromatography using nickel-nitrilotriacetic acid-agarose (Qiagen). The proteins were eluted with 50 mM sodium phosphate buffer (pH 8.0) containing 300 mM NaCl and 250 mM imidazole. Desalting and concentrating the proteins were performed using Centricon YM-30 (Millipore). Finally, the purified proteins were dialyzed against PBS. The method for measuring the protein concentration is described under "Measurement of Soluble ST2 and Cytokines." Deglycosylation with *N*-glycosidase F (Roche Applied Science) was performed as described previously (17). The protein purity was evaluated using a silver staining kit.

Establishment of Stable Cell Lines—Empty vector (pEF6-V5-His) and expression vectors (pEF6-mST2L-FLAG and pEF6-mIL-1RI-FLAG) were linearized with FspI. EL-4 cells (1×10^7 cells) were mixed with 50 μg of linearized plasmid DNA in serum-free RPMI 1640 medium, and the mixtures were left for 10 min on ice. Electroporation was carried out using a Gene Pulser (Bio-Rad) at 270 V and 960 microfarads, and then the cells were left on ice for 10 min. The transfected cells were returned to the RPMI 1640 growth medium and were incubated at 37 °C in 5% CO_2. Forty-eight hours after transfection, the transfected cells were selected with blasticidin (Invitrogen). Stable clones were cultured in RPMI 1640 growth medium containing 6 μg/ml blasticidin.

Flow Cytometry—Splenocytes (1×10^6 cells) and stably transfected EL-4 cells (5×10^5 cells) were used for flow cytometric analysis. Preparation of splenocytes proceeded as follows. The spleen was homogenized into a single-cell suspension in PBS by filtration through nylon mesh (70 μm). After depletion of erythrocytes by osmotic lysis, the splenocytes were washed with PBS and resuspended in PBS containing 5% fetal bovine serum. Subsequently, anti-mouse CD16/CD32 antibody (BD Biosciences PharMingen, San Diego, CA) was mixed with the splenocytes to block the Fc receptor for 5 min on ice. Binding analysis of IL-33 and IL-1β on the cell surface was performed as follows. The cells were mixed with 100 or 500 ng of rIL-33 or rIL-1β for 1 h on ice, followed by staining with biotinylated anti-T7 tag antibody (Novagen) for 1 h on ice. Then the cells were stained with R-phycoerythrin (RPE)-conjugated streptavidin (DakoCytomation, Glostrup, Denmark) for 30 min on ice. In case of binding analysis in the presence of soluble ST2, 1 μg of ST2-V5 was added to the cells at 1 h before, at 1 h after, or at the same time as the addition of rIL-33 or rIL-1β. Binding of ST2-V5 was detected with fluorescein isothiocyanate (FITC)-conjugated anti-V5 antibody (Invitrogen) for 1 h on ice. ST2L or IL-1RI was stained with FITC-conjugated anti-mouse T1/ST2 antibody (MD Biosciences, Zürich, Switzerland), RPE-conjugated anti-mouse IL-1RI antibody (BD Biosciences PharMingen), or each isotype control antibody for 1 h on ice. After the stained cells were washed twice with PBS containing 5% fetal bovine serum, the cells were resuspended in PBS and filtered through nylon mesh (35 μm). Analysis was performed on Becton Dickinson LSR using Cell Quest software (BD Biosciences).

Immunoprecipitation—Five hundred ng of ST2-V5 was mixed with 2 μg of rIL-33 or rIL-1β in 500 μl of RIPA buffer (50 mM Tris-HCl, pH 8.0, 150 mM NaCl, 1% (v/v) Nonidet P-40, 0.5% (w/v) deoxycholate, 0.1% (w/v) SDS), and the mixture was agitated overnight at 4 °C. The protein complexes were immunoprecipitated with 40 μl of 50% (v/v) slurry of anti-T7 tag antibody-conjugated agarose (Novagen). After the protein-bound agarose was washed three times with RIPA buffer, binding protein complexes were eluted with 0.1 M citric acid (pH 2.2) and neutralized with the addition of 2 M Tris (pH 10.4). The eluted proteins were subjected to Western blotting.

Western Blotting—The protein samples were separated by electrophoresis on SDS-polyacrylamide gels. The proteins were transferred to a polyvinylidene difluoride membrane (Millipore) and were probed with mouse monoclonal anti-T7 tag (Novagen), rabbit polyclonal anti-IL-33 (Adipogen Inc., Seoul, South Korea), goat polyclonal anti-IL-1β (Santa Cruz Biotechnology, Santa Cruz, CA), mouse monoclonal anti-V5 (Invitrogen), mouse monoclonal anti-His (C Term) (Invitrogen), rabbit polyclonal anti-IκBα (Santa Cruz), or mouse monoclonal anti-glyceraldehyde-3-phosphate dehydrogenase (Santa Cruz) antibody as the primary antibody. The proteins were detected with

horseradish peroxidase-conjugated goat anti-mouse Ig (Bio-Rad), horseradish peroxidase-conjugated horse anti-goat Ig (Vector, CA), or horseradish peroxidase-conjugated donkey anti-rabbit Ig (Amersham Biosciences) as the secondary antibody. The proteins were visualized using Immobilon Western detection reagents (Millipore), and the membranes were exposed to x-ray films (RX-U; Fuji Photo Film Co., Tokyo, Japan).

Preparation of Cytoplasmic and Nuclear Extracts—Preparation of cytoplasmic and nuclear extracts from stably transfected EL-4 cells was performed as described previously (16). Briefly, the cells were harvested and rinsed with PBS. The cell pellets were resuspended in 5 volumes of a buffer solution (10 mM Hepes-KOH, pH 8.0, 10 mM KCl, 1.5 mM $MgCl_2$, 1 mM dithiothreitol). After addition of Nonidet P-40 to a final concentration of 0.1% (v/v), cytoplasmic extracts were separated by centrifugation. The nuclei were resupended in 2.5 volumes of a buffer solution (20 mM Hepes-KOH, pH 8.0, 420 mM KCl, 1.5 mM $MgCl_2$, 0.2 mM EDTA, 25% (v/v) glycerol, 1 mM dithiothreitol, 0.5 mM phenylmethylsulfonyl fluoride) and mixed by agitation. The debris was removed by centrifugation, and the supernatants were dialyzed against a buffer solution (20 mM Hepes, pH 8.0, 100 mM KCl, 0.2 mM EDTA, 20% (v/v) glycerol, 1 mM dithiothreitol, 0.5 mM phenylmethylsulfonyl fluoride). After centrifugation, the supernatants were harvested as nuclear extracts. The protein concentration was determined by the Bradford method. Cytoplasmic and nuclear extracts were stored at −80 °C until assay.

Electrophoretic Mobility Shift Assay (EMSA)—EMSA was performed as described previously, with some modifications (16, 19). Binding reactions were performed at 30 °C for 30 min in a total volume of 15 μl containing nuclear extracts (5 μg of protein) and 20,000 cpm of ^{32}P-labeled oligonucleotide probe. Supershift assay was carried out using antibodies against p50, p52, p65, and c-Rel (Santa Cruz). The protein-DNA complexes were separated on 4% nondenaturing polyacrylamide gels at 100 V in 0.5 × TGE (50 mM Tris-HCl, pH 8.0, 380 mM glycine, 2 mM EDTA) at 4 °C. The dried gels were exposed to Imaging plates (Fuji Photo Film Co.) and analyzed using Typhoon 9410 (Amersham Biosciences). The oligonucleotide probe containing an NF-κB binding site was created by annealing NF-κB-s (5′-AGTTGAGGGGACTTTCCCAGGC-3′) and NF-κB-as (5′-AGCCTGGGAAAGTCCCCTCAAC-3′).

Luciferase Assay—The luciferase assay was performed as described previously (16). EL-4 cells stably expressing ST2L or IL-1RI (1×10^7 cells) were transfected with plasmid DNAs (40 μg of firefly luciferase reporter plasmid, pNF-κB-Luc, containing an NF-κB binding site in the promoter, and 4 μg of the *Renilla* luciferase reporter plasmid pRL-TK (Promega, Madison, WI)) by electroporation. Twenty-four hours after transfection, the cells were washed and cultured in serum-free medium for 15 h. The transfected cells were treated with 500 ng/ml of ST2-V5 for 3 h, followed by stimulation with 10 ng/ml rIL-33 or rIL-1β for 24 h. Then the cells were harvested and subjected to luciferase assay using a dual luciferase reporter assay system (Promega). Luciferase activity was measured by a luminometer (Lumat LB9507; Berthold Technologies, Bad Wildbad, Germany). The firefly luciferase activity was normalized against the respective *Renilla* luciferase activity.

Stimulation of Splenocytes—Splenocytes were prepared as described under "Flow Cytometry" and resuspended in RPMI 1640 growth medium. Splenocytes (4×10^7 cells/well) were stimulated with 200 μg/ml OVA for 48 h in 6-well plate. The OVA-stimulated cells were washed with PBS and resuspended with serum-free RPMI 1640 medium at 2.5×10^6 cells/well in 48-well plate. After incubation for 15 h, ST2-FLAG was added to a final concentration of 500 ng/ml for 3 h. Then the cells were stimulated with 10 ng/ml rIL-33 or rIL-1β for 48 h. The culture supernatant was harvested and stored at −80 °C until assay.

Measurement of Soluble ST2 and Cytokines—The concentrations of soluble ST2 in sera and purified recombinant proteins were measured by a sandwich enzyme-linked immunosorbent assay (ELISA) as described previously (15). The concentrations of IL-4, IL-5, IL-13, and IFN-γ in culture supernatants were measured using ELISA kits (BIOSOURCE International Inc., Camarillo, CA).

Statistical Analysis—The data are represented as the means ± S.E. The data were analyzed by the Turkey-Kramer test. A value of $p < 0.05$ was considered to be significant.

RESULTS

Specific Binding of IL-33 to ST2L-positive Cells—To study the binding and function of IL-33, we developed systems for the expression and purification of mature IL-33 as a recombinant protein (designated as rIL-33) (Fig. 1*A*). In this study, recombinant mature IL-1β (designated as rIL-1β) was also used for control experiments, because IL-1β has binding activity for IL-1RI, but not for ST2L. Recombinant IL-33 and IL-1β containing T7 and His tags were expressed in bacteria and subjected to affinity purification. The purities of rIL-33 and rIL-1β proteins were examined by silver staining and Western blotting (Fig. 1*A*, *a* and *b*). Although rIL-33 was purified as a single band, the purification product of rIL-1β contained a cleaved product. Next, to establish a clear analysis system for the binding of IL-33, we generated cell lines stably expressing ST2L or IL-1RI using EL-4 cells (Fig. 1*B*). Although ST2L was hardly detected in cells stably transfected with an empty vector (EV/EL-4) or an IL-1RI expression vector (IL-1RI/EL-4), remarkable expression of ST2L was observed in ST2L expression vector-transfected cells (ST2L/EL-4). In addition to a constitutive expression of IL-1RI in EL-4 cells, IL-1RI was further expressed in IL-1RI/EL-4 cells. We examined the binding activity of IL-33 using these stably transfected cell lines (Fig. 1*C*). The ST2L/EL-4 cells clearly shifted according to the increasing concentration of rIL-33 (Fig. 1*C*, *middle panel*). Conversely, EV/EL-4 and IL-1RI/EL-4 cells showed little change corresponding to the expression of ST2L. These results demonstrate that IL-33 specifically binds to ST2L.

Inhibition of IL-33 Binding Activity by Soluble ST2—The amino acid sequence of soluble ST2 except for 9 amino acids in the C terminus is the same as that of the extracellular domain of ST2L (1, 3). Therefore, it seemed possible that soluble ST2 might also bind to IL-33. To investigate this possibility, we generated recombinant soluble ST2 containing either V5 or FLAG and His tags in the C terminus (designated as ST2-V5 or ST2-